Validation of the CMS Cathode Strip Track Finder in the Magnet Test and Cosmic Challenge

Brett Jackson
University of Florida
Gainesville, Florida

Abstract

Validation of the CMS Cathode Strip Chamber (CSC) Track Finder is necessary in the months approaching the Large Hadron Collider becoming operational. The purpose of this study is to assess the performance of the CSC Track Finder during the 2006 Magnet Test and Cosmic Challenge (MTCC), during which cosmic ray muons were measured in one 62º sector of the CSC muon system. The data recorded during these runs were used as the input to the Track Finder Emulator, resulting in emulated tracks. This analysis shows that during the MTCC, all parameter of the tracks found by the online and emulated Track Finders agreed except for the transverse momentum (P_T) and track quality. The assignment of the P_T and track quality depends on the Lookup Tables (LUT) loaded into the CSC Track Finder. The LUT address, used to extract the P_T and quality from the LUT matched in the online and emulated Track Finders, implying the observed differences resulted from different P_T LUTs loaded into the online and emulated Track Finders. With the exception of the P_T and quality, the CSC Track Finder was shown to be in agreement with the Track Finder Emulator, and therefore, validated during the MTCC. A new scheme for parameterizing the contents of the Track Finder LUTs is also described

1. Introduction

1.1. Large Hadron Collider

The Large Hadron Collider (LHC) is currently in the final stages of commissioning, and is scheduled to become operational in summer 2008. The LHC, being constructed at CERN, located outside Geneva, represents the next generation of particle accelerators. The accelerator consists of two circular rings, 27 km in circumference and buried 100 m underground. Figure 1 shows the location of the LHC in relation to the Swiss/France border. The accelerator rings are used to accelerate two proton beams traveling in opposite directions to an unprecedented energy of 7 TeV each. The proton beams are broken up into bunches of 10^{11} protons each. The bunches from the two proton beams are set to cross once every 25 ns. The proton collisions at the LHC will take place at a center-of-mass energy of 14 TeV, and a design luminosity of 10^{34} cm^{-2}s^{-1}. The goal of reaching this unprecedented energy scale is to verify claims made by the Standard Model of Particle Physics, as well as search for signs of new unobserved Physics phenomena.[1]

1.2. The Compact Muon Solenoid

The Compact Muon Solenoid (CMS) is one of the experiments being developed to measure the shower of particles resulting from collisions at the LHC. Diagrams of the CMS detector are show in figures 2 and 3. A solenoid is used to produce a 4 Tesla magnetic field that bends charged particles passing through the detector. The bend of these particles is measured and used to determine the momenta of these particles. CMS is considered to be a general purpose experiment, meaning it can be used in making measurements on a large

range of interaction types, and is not specifically designed for the observation of any single interaction type, such as heavy ion collisions or bottom quark measurements.

CMS is made up of several layers of detector systems. These include the silicon tracker system that tracks the paths of charged particles emitted from the interaction point, the Electromagnetic Calorimeter used in measuring the energy emitted in the form of electrons and photons, the Hadron Calorimeter that measures the energy released in the form of hadrons, and finally the muons systems used to track muons passing through the final layers of the detector. There are in fact three muon systems that make up CMS. These include the Drift Tube Chambers located in the barrel region, the Cathode Strip Chambers (CSCs) located in the endcap regions, and Resistive Place Chambers that are located in both the endcap and barrel regions.[3]

1.2.1. Cathode Strip Chambers

In the two endcap regions, 540 trapezoidal shaped Cathode Strip Chambers (CSC) make up the CSC muon detector system. Each CSC is a 10º or 20º slice of the endcap station filled with a gas that is ionized as a charged particle passes though the chamber. At each endcap, the CSCs are arranged in four stations. Within each station, the CSCs are overlapped to obtain almost 100% coverage of the entire endcap region. Within the four stations of an endcap, the CSCs are further divided into 62º sectors.

The CSCs are made up of anode wires and cathode strips. The combination of anode wires and cathode strips allows for spatial measurements in both the azimuthal angle (ϕ) and the pseudorapidity (η). Pseudorapidity is a measure of the polar angle (θ) and is given by

$$\eta = -\ln\left[\tan\left(\frac{\theta}{2}\right)\right]. \qquad (1)$$

As a charged particle passes through one of the CSCs, the gas within the chamber is ionized. This results in a charge being built up on both the wires and strips. By recording the wire number, it is possible to obtain a measurement for η. To obtain a value for ɸ, the distribution of charge deposited on a layer of strips is read out and fit to the predicted shape of charge distribution. Figure 4 shows a diagram of a charged particle passing though a CSC and depositing charge on a layer of strips as well as an anode wire. Six layers of these strip and wire combinations are included within each CSC in order to improve the spatial resolution. [3]

1.3. Level One Trigger

In an ideal world, it would be possible to record all the data that is taken at CMS, however, due to the sheer volume of data, this is impossible with current technology. Therefore, a trigger system is employed to reduce the amount of data read out of the detector to a manageable amount, while not omitting interesting signs of new Physics. The Level One Trigger is used to make the first cut on data read out from CMS.[4]

1.3.1. CSC Local Trigger And Muon Port Card

The Level One Trigger begins with the onboard electronics called the Cathode Front End Board (CFEB) and the Anode Front End Board (AFEB) that monitor the output of the strips and wires respectively, searching for patterns associated with a muon passing though the chamber. When a pattern is recognized in both the CFEB or AFEB, a Correlated Local Charged Track (LCT) is formed and passed to the Muon Port Card (MPC), which

collects the Correlated LCTs from all CSCs in a given sector and selects the most interesting ones.[4]

1.3.2. CSC Track Finder

The selected Correlated LCTs found in the MPC are passed to the CSC Track Finder. The first stage of the CSC Track Finder is the Sector Receiver. At the Sector Receiver, the LCTs are used to create track segments, which include a value for global ϕ and global η. This global ϕ and global η describe the position of the track segment within its sector. In order to produce track segments from the correlated LCTs, the Sector Receiver uses Sector Receiver Lookup Tables (LUTs) that describe the detector geometry. The input to a LUT is an address defined by a number of parameters such as strip number and wire group number, etc. The data field at that particular address is then used to describe a physical quantity such as the ϕ and η of the track segment. The address and data fields for all the LUTs used in the CSC Track Finder are shown in table 1. The method of using these LUTs to describe the detector geometry is useful because the electronic boards can be reconfigured to use a different geometry simply by loading in a new set of files.

The output of the Sector Receiver is passed on to the Sector Processor (SP). The SP takes the track segments generated in the Sector Receiver and reconstructs tracks, which represent the full path a muon took as it passed through the CSC. In addition to the path taken by the muon, these tracks also contain information regarding the muon's transverse momentum (P_T). The value of P_T as well as a track quality are assigned through the use of another LUT called the P_T LUT. The address and data fields for the P_T LUT are shown in table 1 along with the Sector Receiver LUTs.

One of the words that make up the P_T LUT address is the track mode. The mode is a 4-bit value that describes the stations that contribute to the constructed track. This mode word is used in determining the muon rank., which is used to compare all the muons found in an event. Table 2 gives the definitions of the track modes at the time of the Magnet Test and Cosmic Challenge. The track mode has recently been redefined so the meaning of some modes has changed. The CSCS Track Finder can no longer read in track segments from the second layer of the Muon Barrel region. The new track mode definitions eliminate modes that include the Muon Barrel Layer two, and now include a mode for halo muons, which are muons originating from the accelerator. Table 3 gives the updated definitions of the track modes.[4]

The data field for the P_T LUT also contains a quality word, which is a 2-bit number that, like the track mode, describes the stations contributing to the muon track. Table 4 describes the definition of the track qualities.[5]

1.4. CMS Software Package

While some analysis at CMS is performed in real time for purposes of triggering and data quality management, it is desirable to store the data to a physical medium such as hard disk drives where it can then be distributed to many institutes for full analysis. In order to perform these offline analyses of data taken at CMS, a software framework known as CMS Software (CMSSW) has been developed. The CMSSW framework consists of over 1000 software packages that provide the user tools with which to perform simulated event generation and data analysis.

1.4.1. Software Emulation of Level One Trigger

In order to test the configuration and performance of the Level One Trigger, the entire trigger system has been emulated within CMSSW. The Level One Trigger Emulator uses C++ code to exactly reproduce the actual hardware discussed in section 1.3. Also, whenever the firmware installed in the detector hardware is upgraded, the changes are reflected in the emulation code. The trigger emulator is a useful tool because it can be used with simulated data, generated using Monte Carlo methods, to test new configurations and firmware updates before their implementation into the actual detector. The trigger emulator is also used to validate CSC Track Finder configurations and to check for miscabling of links used to read data from the CSC. For the purposes of this study, the primary concern is the CSC Track Finder. The method for validating the configuration of the CSC Track Finder is discussed in section 4.1.

1.4.2. Software Emulation of the CSC Track Finder

As with the rest of the trigger emulator, the emulation of the CSC Track Finder employs C++ code to reproduce the electronics installed on CMS within the framework of CMSSW. The CSC Track Finder Emulator reads in LCTs found by the actual detector or produced using a Monte Carlo simulation. At this point, the emulator follows the same procedure as the Track Finder implemented in the Sector Receiver and Sector Processor; the emulator uses these LCTs to produce track segments, and then tracks. Finally, the tracks with the highest rank are selected and added to an event, which can ultimately be stored or used in further analysis within the current CMSSW job.

2. Preparation For Collisions

In preparation for data taking at CMS, simulated data as well as cosmic ray muons are used to determine the performance of the detector. Monte Carlo simulations allow for the generation of a large range of physics events including hadron interactions at the collision point. Event simulation allows the user to manually set the type of interaction taking place, and also provides access to the true history of particles produced within the detector. This is advantageous when developing a search for a specific interaction because it is possible to isolate interactions that contribute to the signal of interest as well as the noise. Cosmic ray muons, on the other hand, produce real interactions within the detector that can be measured and observed. Observations of these cosmic rays provide measurements that are used to test the performance and calibration of the actual detector systems that make up CMS, in addition to the software used in data analysis.

3. Magnet Test and Cosmic Challenge

The Magnet Test and Cosmic Challenge (MTCC) are a set of runs during 2006 where data was taken at CMS. The MTCC was the first time in which components of all the detector systems were brought together and used for recording cosmic ray muons in a global run. During a global run, all detector systems are being read out. During the MTCC, one sector of the CSC muon system was active. Within this sector, stations 1, 2, and 3 were operational. [6]

4. Analysis of MTCC Data

4.1. Methods

The purpose of this study is to validate the CSC Track Finder during the MTCC by comparing the output of the online CSC Track Finder to that of the Track Finder Emulator. If the emulator is configured to match the Track Finder electronics, identical tracks should be found in both the online and emulated CSC Track Finders. For this validation study, LCTs recorded during the MTCC Run Number 461 were used as input to the CSC Track Finder Emulator, and then used to generate tracks. The tracks found by the Track Finder Emulator were compared to those found by the online CSC Track Finder. In this comparison, the number of tracks found per event, relative track timing, and track position (η and ϕ) were compared. The transverse momentum (P_T) and track quality assigned to tracks found in the hardware and emulator were also compared.

4.2. Configuration of the Track Finder Emulator

For this analysis to produce meaningful results, the Track Finder Emulator must be configured with the same geometry as online Track Finder. As discussed in the 1.3.2, the geometry is defined by loading a particular version of LUTs. The Sector Receiver LUTs loaded into the Track Finder Emulator were generated within CMSSW_1_0_0, while the P_T LUT was generated within the older CMS framework, Object-oriented Reconstruction for CMS Analysis (ORCA).

9

4.3. Tracks From the Online Hardware

The output from the online CSC Track Finder was read out, and then unpacked to a format that is useful for analysis using CMSSW. For each event within the run, the number of tracks was counted. The tracks' relative timing within the event, position within the sector, P_T, and quality were recorded. Figures 5 through 10 show these distributions as observed in the unpacked data from the detector.

Figure 5 shows that most events result in either one or no tracks found. There are also events with two or three tracks found, however these occur far less often.

Figure 6 shows that the relative timing distribution is centered at bunch crossing zero. This should be the case by design, when the CSC self-triggers, or external an external trigger is synchronized to the CSC trigger. The CSC trigger allows for a window of seven bunch crossings, which make up a single event. When a trigger occurs, the event window is set to include the three bunch crossings before and after the trigger. This means that most tracks should occur at bunch crossing zero. It is possible for the second or third track in an event to occur before or after zero.

Figures 7 and 8 show the distributions of ϕ and η for tracks observed in the online CSC Track Finder. The η distribution is within a range of 1 to 2.4 because only the positive endcap was used during the MTCC run, and this range in η covers almost all of the CSC region within the positive endcap.

Figure 9 shows the distribution of the P_T observed by the online CSC Track Finder. There is a large number of low P_T muons, as well as a small number of muons with P_T of 31

which means the muon passed through the detector with no detectable bend. The large spike in the P_T distribution at 5 is a result of tracks with a quality of 1. Quality 1 corresponds to tracks with no track segment in Station 1, or in the Muon Barrel Layer 1. These tracks have a poor P_T resolution, and the current P_T assignment algorithm forces the P_T value of these tracks to 5 corresponding to a transverse momentum of 3 GeV.

Figure 10 shows the quality of tracks found by the online CSC Track Finder. These values of track quality correspond to the definitions shown in table 4.

4.4. Tracks From the Software Emulation

As with the online CSC Track Finder, the output from the CSC Track Finder Emulator was read out, and analyzed event by event. Again, the number of tracks was counted. The relative timing, track location in the sector, P_T, and quality were also recorded for each event. These distributions recorded from the output of the Track Finder Emulator are shown in figures 11 through 16.

Figures 11 through 14 have similar distributions to the figures 5 through 8. While this is not conclusive evidence that the output of the Track Finder Emulator matches with the data unpacked from the hardware output, it suggests that the two outputs are at least similar. This is investigated in greater depth in the following section.

Figures 15 and 16 show the distributions of P_T and track quality found by the Track Finder Emulator. These distributions do not appear to match very well with the plots shown in figures 9 and 10. This suggests that the outputs are different. These differences are discussed in the next section.

4.5. Comparison of Tracks From Hardware and Emulator

Using the plots discussed in sections 4.3 and 4.4 it is possible to compare the distribution of various observables such as number of tracks, timing, position, etc. This can be used to detect obvious differences, however, these plots cannot be used as evidence that the emulator and hardware are in fact a perfect match. It was desired to look at the events more closely and compare the tracks on an event-by-event basis, to ensure that every event matches exactly.

For each event, the number of tracks found were compared, and plotted. Figure 17 shows a comparison of the number of tracks found by the online Track Finder (unpacker) and the Track Finder Emulator, where the relative size of the box is proportional to the number of counts in that particular bin. In this plot, entries along the diagonal line starting at the origin correspond to events where the number of tracks found in the hardware and emulator match. Any discrepancy in the number of tracks found by the online Track Finder and the Track Finder Emulator would result in an entry to the plot that is off this diagonal line. Figure 17 shows that for all events in this run, the Track Finder Emulator and the online Track Finder found the same number of tracks.

For events where the hardware and emulator find the same number of tracks, the found tracks are passed on to be further compared. Otherwise, the event is listed as a mismatch, and disregarded for this analysis. It is possible to perform a comparison for these events with a mismatch in the number of tracks; however, this would require a more sophisticated track-matching algorithm to select the tracks to be compared. In this

particular run, the hardware and emulator agree on the number of tracks found in all events, so this is not necessary.

For each event when the number of tracks found in the hardware and the emulator Track Finders match, the variables discussed in sections 4.2 and 4.3, which include the relative timing, ϕ, η, P_T, and track quality, were compared and plotted. These plots are shown in figures 18 through 22. As with the plot in figure 17, the relative size of the box is proportional to the number of counts within the bin, and any mismatches between the tracks found in hardware and the track found in the emulator result in an entry that is off the diagonal line running through the origin.

The comparison plots of relative timing, ϕ, and η are shown in figures 18, 19, and 20 respectively. These plots show that for the tracks found in the online Track Finder and in the Track Finder Emulator, these three observable quantities match for all events.

Figures 21 and 22 show the comparison between the P_T and quality assigned to tracks found in the online Track Finder and in the Track Finder Emulator. As suggested earlier, these plots show that the P_T and quality assigned to tracks found by the Track Finder Emulator differ from those found by the online Track Finder.

4.5.1. Disagreement in P_T and Track Quality

In an attempt to explain the disagreement in P_T and quality assignment observed in the online and emulated Track Finders, the P_T LUT address was read out and plotted for all events. As shown in table 1, the P_T LUT address has five component words. There is also a front/rear (f_r) bit that is set by the Sector Processor. While the f_r bit is not actually part

of the P_T LUT address, it is used in assigning the track P_T and quality. For this reason the f_r

bit is also plotted as a possible cause for disagreements in track P_T and quality. Figures 23

and 24 show the distributions of the P_T LUT address components. Figure 25 shows a

comparison for each of these address components. The plots in figure 25 show that the

component words for the P_T LUT address match for all events, meaning the whole P_T LUT

address, also matches for all events. This is very important to note because it implies that

although the values read out for the P_T and quality do not match, the LUT address that

determines their location within the P_T LUT does in fact match. This suggest the P_T LUT

loaded into the emulator does not match with the one used during the MTCC.

5. Tracking Changes in Lookup Tables

This study has highlighted the important role Lookup Tables (LUTs) play in the CSC

Track Finder performance. By making changes to the LUTs, one is changing the geometry

modeled within the CSC Track Finder, which can potentially have a great impact on the

tracks found. For many upgrades of the CMSSW framework, the geometry modeled by

these LUTs remain the same; however, when changes do occur, it is desired to understand

the changes and ensure they are then implemented into the online CSC Track Finder.

During the course of this study a tool was developed to this effect.

The analysis tool allows the user to compare the Sector Receiver LUTs and the P_T

LUT of the current CMSSW release with those generated using a previous version of the

framework. This comparison tool allows for a visual way to view these change from

release-to-release.

For this comparison routine, the user can specify the version of LUTs with which to compare the LUTs from the current release. The user can also select the endcap, sector, station, and subsector (in station 1) over which to compare the LUTs.

The program loops over all addresses in the LUTs specified by the user. For each address, the data fields of the two LUTs are compared in a temperature plot. The component words of the data fields shown in table 1 are also compared in a temperature plot. Examples of these plots obtained by comparing LUTs from CMSSW_1_8_0 with those generated in CMSSW_1_7_4 are shown in figures 26 through 32.

The input to the Local ϕ LUT includes the pattern ID and pattern # words. The pattern ID is the key half strip that is defined by the Cathode Front End Board (CFEB). The Pattern # describes path traveled by a muon as it passes through the six layers within a CSC. The Pattern # is used to assign an offset to the pattern ID in order to improve the strip assignment to achieve the best strip value based on all six layers. The output of the Local ϕ LUT is a 10-bit data field describing the angular position within the CSC.

Figure 26 shows the comparison of the Phi Local word of the Local ϕ LUT. The Phi Local word is the only component of the Local ϕ LUT data field that is compared because the Phi Bend Local word has not yet been implemented. When this word is implemented, it will also be compared to previous version of the Local ϕ LUT.

The input to the Global η ME LUT includes the wire group from the Anode Front End Board (AFEB) and the CSC number. The output of this LUT is a 7-bit word that describes the value of η over a range of 0.9 to 2.5.[3] The binning in the reported η is 0.0125. It should also be noted that in Station 1, the η scale is non-linear near 1.6. This non-linearity

is put in place to remove the overlap between the Ring 1 and Ring 2 of Station 1. Due to this non-linearity, the value of Global η can be used to determine the Ring of CSCs because there is no overlap in the reported value of η.

Figure 27 shows the comparison of the Eta Global word of the Global η ME LUT for endcap 1/sector 1/station 2. The Eta Global word is the only component of the data field that is compared in this plot because the Phi Bend Global word has also not been implemented.

The Global ɸ ME LUTs read in the Local ɸ and CSC. These are used to compute a 12-bit word that describes the angular position within the entire 62º sector. The wire group is also read in as an input parameter to the Global ɸ ME LUT. The wire group is used when correcting for misalignment that may be present.

Figure 28 shows the comparison of the Global ɸ ME LUT for endcap 1/sector 1/station 2. The entire data field for the Global ɸ ME LUT is compared because it only consists of a single word describing the azimuthal angle in the endcap region.

Figures 26 through 28 only contain entries along the diagonal line signifying matching data fields. This shows that, at least for Local ɸ and endcap 1/sector 1/station 2, the Sector Receiver LUTs remain the same in CMSSW_1_7_4 and CMSSW_1_8_0. The same can be shown for the remaining Sector Receiver LUTs not shown in these plots.

Figure 29 shows the comparison of the P_T LUT data field. It can be seen that there is an area of this plot containing entries that are off the diagonal line signifying matching data

fields. This is a signal to the user that a change in the P_T LUT occurred from CMSSW_1_7_4 to CMSSW_1_8_0.

In order to determine the changes made in the P_T LUT, the comparison routine also plots the LUT addresses that contribute to the off diagonal entries shown in figure 29. A plot of the P_T LUT addresses where mismatches in the data field occur is shown in figure 30. This shows two fairly narrow regions in the LUT address where mismatches occur. The P_T LUT address can be further broken down into its component words as was done in section 4.5.1. In figure 31, the P_T LUT addresses where the mismatches occur are broken down into their component words and plotted. These plots show a flat distribution in Delta12 Phi, Delta23 Phi, Eta, and Sign. On the other hand, the mismatches only occur for a single track mode, mode 15. This particular change in the P_T LUT data fields is due to the change in track mode definition discussed in section 1.3.2, where the definition of mode 15 was changed to represent a halo muon.

For every new release of CMSSW, this LUT comparison program is used to perform a similar analysis, searching for possible changes to the detector geometry within the CMSSW framework.

8. Alignment Corrections In ϕ Coordinate

As mentioned in section 7, the Global ϕ ME LUT is used to make alignment corrections in the ϕ coordinate. It is possible that there may be a small offset in the position of the endcap stations. This offset would most likely be in the X-Y plane defined to be perpendicular to the beam direction. Offsets in the X-Y plane would result in an error in the resulting Global ϕ used in making momentum calculations.

It was shown that the corrected Global ɸ can be computed using

$$\varphi = \tan^{-1}\left[\frac{2ze^{-\eta}\sin\left(\varphi_m + (setor - 1)\cdot 60^o + 14^o\right) + \Delta Y\left(1 - e^{-2\eta}\right)}{2ze^{-\eta}\cos\left(\varphi_m + (setor - 1)\cdot 60^o + 14^o\right) + \Delta X\left(1 - e^{-2\eta}\right)}\right], \quad ,(2)$$

where is the φ_m is the measured value of Global ɸ, and φ is the corrected value of Global ɸ. ΔX and ΔY are offsets added to the measured coordinates to correct for misalignment in the X and Y coordinates respectively. z is the distance from the collision point along the beam line axis, and is determined by the station as well as the CSC number.

7. Parameterization of the Lookup Tables

A concern that has recently been brought up is the memory requirement of the LUTs that are loaded into the CSC Track Finder. The total amount of memory taken up by the LUTs is approximately 164 MB. This is a substantial memory requirement, especially when analysis jobs are distributed across many computers, each having to load the LUTs into memory. An effort has been made to define the Sector Receiver LUTs in terms of parameterized functions, especially Global η ME, Global ɸ ME, and Global ɸ MB. This would substantially reduce the memory requirements of the LUTs. Currently, the parameterization of the Global ɸ LUTs (Muon Endcap and Muon Barrel) requires only two floating-point parameters per CSC. The parameterization of the Global η ME LUT currently requires five floating-point parameters per combination of CSC and the upper two bits of Phi Local. This leads to 18 floating point parameters per Sector Receiver for the Global ɸ LUTs, and 180 floating point parameters per Sector Receiver for the Global η LUTs. This is dramatically different than the standard Sector Receiver LUTs, each of which includes 2^{19} short integer values per Sector Receiver. It should be noted that the number of parameters

required to recreate the LUTs will increase as additional words within the LUT addresses are implemented. The cost of this savings in memory usage is extra clock cycles required to compute the data field from the parameters. This extra CPU requirement is within reason because the calculations are not processor intensive.

The Global ɸ LUTs for both the Muon Endcap region and Muon Barrel region were fit to

$$\phi_{global} = P_0 + P_1 \cdot \phi_{local},$$ (3)

where P_0 and P_1 are fitting parameters. Equation 3 was fit to the data field entries for each CSC of the Global Phi LUTs using the Root software package to perform the regression analysis.

Figure 32 shows the Global Phi ME LUT data field versus ϕ_{local} for each of the CSCs within Endcap 1/Sector 1/Station 1a, where Station 1a is one of the subsectors within station 1. Figure 32 also shows the parameterized curves found by fitting equation 3 to the Global ɸ LUT data field in each CSC. The values for the parameters P_0 and P_1 obtained from the regression analysis of Global ɸ ME for the CSCs in endcap 1/sector 1 are shown in table 5.

The Global ɸ MB LUT data field was plotted versus ϕ_{local} for each of the CSCs within Endcap 1/Sector 1/Station 1a. These plots are shows in figure 33. The plots in figure 33 also show the parameterized curves obtained by fitting equation 3 to the data fields for each CSC. The data fields shown in figure 33 contain negative values. For storage, the Global ɸ LUT data fields are required to fit in a 12-bit field that is not designed to handle

negative numbers. The two's complement is used to represent a negative number as a large positive value. For the case of a 12-bit data field, the negative numbers are represented as positive number greater than 2047. Negative values within the Global ɸ MB LUTs are represented by their two's complement in order to store them in an unsigned data field. Likewise, when generating the plots of Global ɸ MB versus ϕ_{local} shown in figure 33, and when fitting equation 3 to these data, negative values are recovered by taking the two's complement of any data field greater than 2047. When using the parameterized equations to generate the contents of the Global ɸ MB LUT, a conditional statement is used to check the sign of the calculated value. If this calculated value is less than zero, its two's complement is returned instead. The method for taking the two's complement of a 12-bit data field is described in appendix A2. Table 6 shows the fitted parameters P_0 and P_1 from the regression analysis of Global ɸ MB for the CSCs in endcap 1/sector 1.

While the Global ɸ LUTs could be fit to a linear equation, Global η is not linear with wire group. Wire group can be taken as proportional to the tangent of the polar angle (θ). As seen in equation 1, this is not the case with η. The parameterized function used to fit to the Global Eta ME data fields is

$$\eta_{global} = P_0 + P_1 \cdot \ln(P_2 + WG),\qquad(4)$$

where P_0, P_1, and P_2 are fitting parameters, and WG is the wire group. In addition to the increased complexity in calculating Global η from these fitting parameters, the regression must be performed for four possible values of Local Phi. Since the anode wires run straight across the CSCs, they are not at a constant value of η throughout their length. This is even worse in Station 1, where the wires run through the CSCs at an angle of 25º.[3] This makes

20

fitting to Global η a more difficult task than the Global φ. Nonetheless, these curve fits were performed using Root, and these plots of the parameterized functions for the CSCs in endcap 1/sector 1/staion 1a are shown in figure 34. In figure 34, it can also be seen that the value of global η has a maximum and minimum point, after which the values of the data field is held constant. These maximum and minimum values of η are stored as additional parameters to be used when computing global η. Table 7 shows the fitted parameters found for endcap 1/sector 1/station 1a when equation 4 was fitted to the Global η ME LUT in these CSCs.

These parameterized LUTs are being implemented into CMSSW, as an alternate method of reading in the LUTs. It is likely that in the near future, these parameterizations will be further tuned to reach an even better match with the standard LUTs. Depending on the success of this endeavor, it is possible for these parameterized LUTs to be more widely used due to the reduced memory requirements.

8. Conclusion

Based on this analysis, the CSC Track Finder was shown to be in agreement with the Track Finder Emulator for most parameters of interest during the 2006 Magnet Test and Cosmic Challenge (MTCC). By comparing the tracks found in both the hardware and emulator, it was shown that the number of event found, relative timing, azimuthal angle (φ), and pseudorapidity (η) agree exactly. The transverse momentum (P_T) and track quality found in the emulator however, do not match those found in hardware. By comparing the P_T LUT addresses that are used to find the values for P_T and quality, it was determined that the mismatch in these parameters resulted from a different P_T LUT used in

the online and emulated CSC Track Finders. Unfortunately, the P_T LUT used during the MTCC was not available for use in the offline analysis. These results validate the ability of the CSC Track Finder to reconstruct muon tracks, with the exception of the PT and quality assignment, which can be corrected by updating the P_T LUT.

Acknowledgements

I am indebted to many people whose support has made this work, as well as the completion of my Bachelor's degree at the University of Florida possible. First and foremost, I would like to thank my parents David and Brenda Jackson. Throughout my five years at the University of Florida, they have stood by me, with their unconditional love and support.

I would like to thank Professor Darin Acosta, who has guided me through my career as an undergraduate research assistant. He has taught me how to approach problems, and has also been a patient teacher while explaining various aspects of this experiment. I would also like to thank the rest of CSC Track Finder Group, especially Joseph Gartner, Dan Holmes, and Khristian Kotov. They have provided me with much assistance during the developing this analysis.

Finally, I thank the faculty in the University of Florida Department of Physics, who have played a vital role in teaching me the basics of Physics. This preparation has instilled a confidence in me that has allowed me to approach problems, knowing I have been trained the skills necessary for the task. The influence from the faculty I have interacted with during my time at the University of Florida has reinforced my desire to contribute to the scientific community as I continue my journey though my academic career.

Appendix A1: Glossary of Acronyms

AFEB: Anode Front End Board

CFEB: Cathode Front End Board

CMS: Compact Muon Solenoid

CMSSW: CMS Software

CSC: Cathode Strip Chamber

f_r bit: Front/Rear bit

LCT: Local Charged Track

LHC: Large Hadron Collider

LUT: Lookup Table

MB: Muon Barrel

ME: Muon Endcap

MPC: Muon Port Card

MTCC: Magnet Test and Cosmic Challenge

ORCA: Object-Oriented Reconstruction for CMS Analysis

SP: Sector Processor

Appendix A2: Two's Complement

The two's complement of an 12-bit data field X is given by

$$2's(X) = \left[\sim(X) + 1\right] \& \, 0\text{xfff} .$$

The $\sim$ operator represents the one's complement where all the bits within the value X are flipped between 0 and 1. The & operator is the bitwise and operator. The & operator is used to protect the resulting value from bit overflows that may occur while taking the two's complement.

References

[1] B. Scurlock, "Compact Muon Solenoid Discovery Potential For the Minimal Supergravity Model of SuperSymmetry in Single Muon Events With Jets And Large Missing Transverse Energy In Proton-Proton Collisions at Center-of-Mass Energy 14 TeV," http://tier2.ihepa.ufl.edu/~bslock/thesis/Thesis.pdf

[2] photo-lhc/lhc-pho-1997-237

[3] CMS, The Muon Project Technical Design Report , CERN/LHCC 97-32

[4] CMS, The TriDAS Project Technical Design Report, Volume 1, CERN/LHCC 2000-38

[5] D. Acosta, M. Stoutimore, S.M. Wang, "Simulated Performance of the CSC Track-Finder," CMS NOTE 2001/033

[6] D. Acosta et al., "The Cathode Strip Track Finder at the 2006 Magnet Test and Cosmic Challenge," CMS IN 2005/000

Table 1: Address and data fields for the Sector Receiver LUTs and the P_T LUT.

Local Phi LUT 512K x 16

LP_A18	Spare
LP_A17	Spare
LP_A16	Left/Right
LP_A15	Quality_3
LP_A14	Quality_2
LP_A13	Quality_1
LP_A12	Quality_0
LP_A11	CLCT Pattern #_3
LP_A10	CLCT Pattern #_2
LP_A9	CLCT Pattern #_1
LP_A8	CLCT Pattern #_0
LP_A7	CLCT Pattern ID_7
LP_A6	CLCT Pattern ID_6
LP_A5	CLCT Pattern ID_5
LP_A4	CLCT Pattern ID_4
LP_A3	CLCT Pattern ID_3
LP_A2	CLCT Pattern ID_2
LP_A1	CLCT Pattern ID_1
LP_A0	CLCT Pattern ID_0
LP_D15	PhiBend Local_5
LP_D14	PhiBend Local_4
LP_D13	PhiBend Local_3
LP_D12	PhiBend Local_2
LP_D11	PhiBend Local_1
LP_D10	PhiBend Local_0
LP_D9	Phi Local_9
LP_D8	Phi Local_8
LP_D7	Phi Local_7
LP_D6	Phi Local_6
LP_D5	Phi Local_5
LP_D4	Phi Local_4
LP_D3	Phi Local_3
LP_D2	Phi Local_2
LP_D1	Phi Local_1
LP_D0	Phi Local_0

Global Eta LUT 512K x 16

GE_A18	CSC ID_3
GE_A17	CSC ID_2
GE_A16	CSC ID_1
GE_A15	CSC ID_0
GE_A14	Wire Group ID_6
GE_A13	Wire Group ID_5
GE_A12	Wire Group ID_4
GE_A11	Wire Group ID_3
GE_A10	Wire Group ID_2
GE_A9	Wire Group ID_1
GE_A8	Wire Group ID_0
GE_A7	Phi Local_9
GE_A6	Phi Local_8
GE_A5	PhiBend Local_5
GE_A4	PhiBend Local_4
GE_A3	PhiBend Local_3
GE_A2	PhiBend Local_2
GE_A1	PhiBend Local_1
GE_A0	PhiBend Local_0
GE_D15	not connected
GE_D14	not connected
GE_D13	not connected
GE_D12	not connected
GE_D11	PhiBend Global_4
GE_D10	PhiBend Global_3
GE_D9	PhiBend Global_2
GE_D8	PhiBend Global_1
GE_D7	PhiBend Global_0
GE_D6	Eta Global_6
GE_D5	Eta Global_5
GE_D4	Eta Global_4
GE_D3	Eta Global_3
GE_D2	Eta Global_2
GE_D1	Eta Global_1
GE_D0	Eta Global_0

Global Phi LUT 512K x 16

GP_A18	CSC ID_3
GP_A17	CSC ID_2
GP_A16	CSC ID_1
GP_A15	CSC ID_0
GP_A14	Wire Group ID_6
GP_A13	Wire Group ID_5
GP_A12	Wire Group ID_4
GP_A11	Wire Group ID_3
GP_A10	Wire Group ID_2
GP_A9	Phi Local_9
GP_A8	Phi Local_8
GP_A7	Phi Local_7
GP_A6	Phi Local_6
GP_A5	Phi Local_5
GP_A4	Phi Local_4
GP_A3	Phi Local_3
GP_A2	Phi Local_2
GP_A1	Phi Local_1
GP_A0	Phi Local_0
GP_D15	not connected
GP_D14	not connected
GP_D13	not connected
GP_D12	not connected
GP_D11	Phi Global_11
GP_D10	Phi Global_10
GP_D9	Phi Global_9
GP_D8	Phi Global_8
GP_D7	Phi Global_7
GP_D6	Phi Global_6
GP_D5	Phi Global_5
GP_D4	Phi Global_4
GP_D3	Phi Global_3
GP_D2	Phi Global_2
GP_D1	Phi Global_1
GP_D0	Phi Global_0

=

DT Phi LUT 512K x 16 — ME1 Muons Only

DT_A18	CSC ID_3
DT_A17	CSC ID_2
DT_A16	CSC ID_1
DT_A15	CSC ID_0
DT_A14	Wire Group ID_6
DT_A13	Wire Group ID_5
DT_A12	Wire Group ID_4
DT_A11	Wire Group ID_3
DT_A10	Wire Group ID_2
DT_A9	Phi Local_9
DT_A8	Phi Local_8
DT_A7	Phi Local_7
DT_A6	Phi Local_6
DT_A5	Phi Local_5
DT_A4	Phi Local_4
DT_A3	Phi Local_3
DT_A2	Phi Local_2
DT_A1	Phi Local_1
DT_A0	Phi Local_0
DT_D15	not connected
DT_D14	not connected
DT_D13	not connected
DT_D12	not connected
DT_D11	DT Phi Global_11
DT_D10	DT Phi Global_10
DT_D9	DT Phi Global_9
DT_D8	DT Phi Global_8
DT_D7	DT Phi Global_7
DT_D6	DT Phi Global_6
DT_D5	DT Phi Global_5
DT_D4	DT Phi Global_4
DT_D3	DT Phi Global_3
DT_D2	DT Phi Global_2
DT_D1	DT Phi Global_1
DT_D0	DT Phi Global_0

PT LUT 2M x 16

PT_A20	Sign
PT_A19	Mode_3
PT_A18	Mode_2
PT_A17	Mode_1
PT_A16	Mode_0
PT_A15	Eta_3
PT_A14	Eta_2
PT_A13	Eta_1
PT_A12	Eta_0
PT_A11	Delta23 Phi_3
PT_A10	Delta23 Phi_2
PT_A9	Delta23 Phi_1
PT_A8	Delta23 Phi_0
PT_A7	Delta12 Phi_7
PT_A6	Delta12 Phi_6
PT_A5	Delta12 Phi_5
PT_A4	Delta12 Phi_4
PT_A3	Delta12 Phi_3
PT_A2	Delta12 Phi_2
PT_A1	Delta12 Phi_1
PT_A0	Delta12 Phi_0
PT_D15	R Valid Charge
PT_D14	R Quality_1
PT_D13	R Quality_0
PT_D12	R Rank_4
PT_D11	R Rank_3
PT_D10	R Rank_2
PT_D9	R Rank_1
PT_D8	R Rank_0
PT_D7	F Valid Charge
PT_D6	F Quality_1
PT_D5	F Quality_0
PT_D4	F Rank_4
PT_D3	F Rank_3
PT_D2	F Rank_2
PT_D1	F Rank_1
PT_D0	F Rank_0

Table 2: Definition of track modes at the time of the Magnet Test and Cosmic Challenge. In this table, ME stands for Muon Endcap, and MB means Muon Barrel.

Mode	Track Type
0	No μ
1	A Match bit unset (only for 3-station tracks)
2	ME1-ME2-ME3
	ME1-ME2-ME3-ME4
3	ME1-ME2-ME4
4	ME1-ME3-ME4
5	ME2-ME3-ME4
6	ME1-ME2
7	ME1-ME3
8	ME2-ME3
9	ME2-ME4
a	ME3-ME4
b	MB1-MB2-ME2
	MB1-MB2-ME1-ME2
c	MB1-ME1-ME2
d	MB2-ME1-ME2
e	MB1-ME2
f	MB2-ME2

Table 3: Updated definitions of track modes. The new track mode definitions also allocate a value for a halo muon. In this table, ME stands for Muon Endcap, and MB means Muon Barrel.

Mode	Track Type
0	No μ
1	A Match bit unset (only for 3-station tracks)
2	ME1-ME2-ME3
	ME1-ME2-ME3-ME4
3	ME1-ME2-ME4
4	ME1-ME3-ME4
5	ME2-ME3-ME4
6	ME1-ME2
7	ME1-ME3
8	ME2-ME3
9	ME2-ME4
a	ME3-ME4
b	Unused
c	MB1-ME1-ME2
d	Unused
e	MB1-ME2
f	Halo μ

Table 4: Definitions of track quality. In this table, ME stands for Muon Endcap, and MB means Muon Barrel.[6]

Quality	Meaning
0	No Track
1	Track in the DT/CSC overlap region without track segment in MB1
1	Track in the CSC Region without a track segment in ME1
2	Two-station tracks with a track segment in ME1 or MB1
2	Three-station track of type ME1-ME3-ME4
3	Three or four station track with a track segment in ME1 or MB1, ME2, and ME3 or ME4

Table 5: Fitting parameters used in calculating Global ϕ ME using the parameterized equation 3. These parameters were found for sector 1 of station 1.

Station	CSC	P0	P1
1a	1	37.99	0.8748
1a	2	698.7	0.8748
1a	3	1359	0.8748
1a	4	41.25	0.6890
1a	5	701.9	0.6890
1a	6	1363	0.6890
1a	7	132.5	0.6387
1a	8	793.2	0.6388
1a	9	1454	0.6387
1b	1	2020	0.8748
1b	2	2681	0.8748
1b	3	3341	0.8748
1b	4	2023	0.6890
1b	5	2684	0.6890
1b	6	3344	0.6890
1b	7	2114	0.6387
1b	8	2775	0.6388
1b	9	3436	0.6388

Table 6: Fitting parameters used in calculating Global ɸ MB using the parameterized equation 3. These parameters were found for sector 1 of station 1.

Station	CSC	P_0	P_1
1a	1	-1108	0.9517
1a	2	-389.8	0.9516
1a	3	328.9	0.9516
1a	4	-1105	0.7495
1a	5	-386.3	0.7496
1a	6	332.4	0.7496
1a	7	-1006	0.6949
1a	8	-287.0	0.6949
1a	9	431.7	0.6949
1b	1	-1109	0.9516
1b	2	-389.8	0.9516
1b	3	328.8	0.9516
1b	4	-1105	0.7496
1b	5	-386.3	0.7496
1b	6	332.4	0.7495
1b	7	-1006	0.6949
1b	8	-287.0	0.6949
1b	9	431.6	0.6949

Table 7: Fitting parameters used in calculating Global η ME using the parameterized equation 4. These parameters were found for sector 1 of station 1a.

Local φ	CSC	P0	P1	P2	Min η	Max η
1	1	357.7	-69.14	28.90	57	122
1	2	355.2	-69.32	29.49	56	118
1	3	357.7	-69.15	28.90	57	122
1	4	1711	-268.7	466.8	26	54
1	5	4278	-602.7	1102	23	54
1	6	1711	-268.7	466.8	26	54
1	7	200.9	-43.67	68.95	0	15
1	8	200.9	-43.67	68.95	0	15
1	9	200.9	-43.67	68.95	0	15
2	1	356.1	-69.13	29.46	56	120
2	2	342.3	-67.07	28.28	56	115
2	3	356.1	-69.13	29.46	56	120
2	4	2472	-371.4	661.3	26	54
2	5	3846	-548.4	1002	23	54
2	6	2472	-371.4	661.3	26	54
2	7	263.5	-54.97	89.95	0	15
2	8	263.5	-54.97	89.95	0	15
2	9	263.5	-54.97	89.95	0	15
3	1	338.6	-66.08	27.26	56	117
3	2	350.2	-69.25	29.79	56	113
3	3	338.6	-66.05	27.26	56	117
3	4	2982	-438.2	787.7	26	54
3	5	3846	-548.4	1002	23	54
3	6	2982	-438.2	787.7	26	54
3	7	270.7	-56.12	93.75	0	15
3	8	270.7	-56.12	93.75	0	15
3	9	270.7	-56.12	93.75	0	15
4	1	327.3	-64.00	26.20	56	115
4	2	312.6	-61.72	24.89	56	111
4	3	327.3	-64.00	26.20	56	115
4	4	1711	-268.7	466.8	26	54
4	5	4278	-602.7	1102	23	54
4	6	1711	-268.7	466.8	26	54
4	7	211.9	-45.83	71.73	0	15
4	8	211.9	-45.83	71.73	0	15
4	9	211.9	-45.83	71.73	0	15
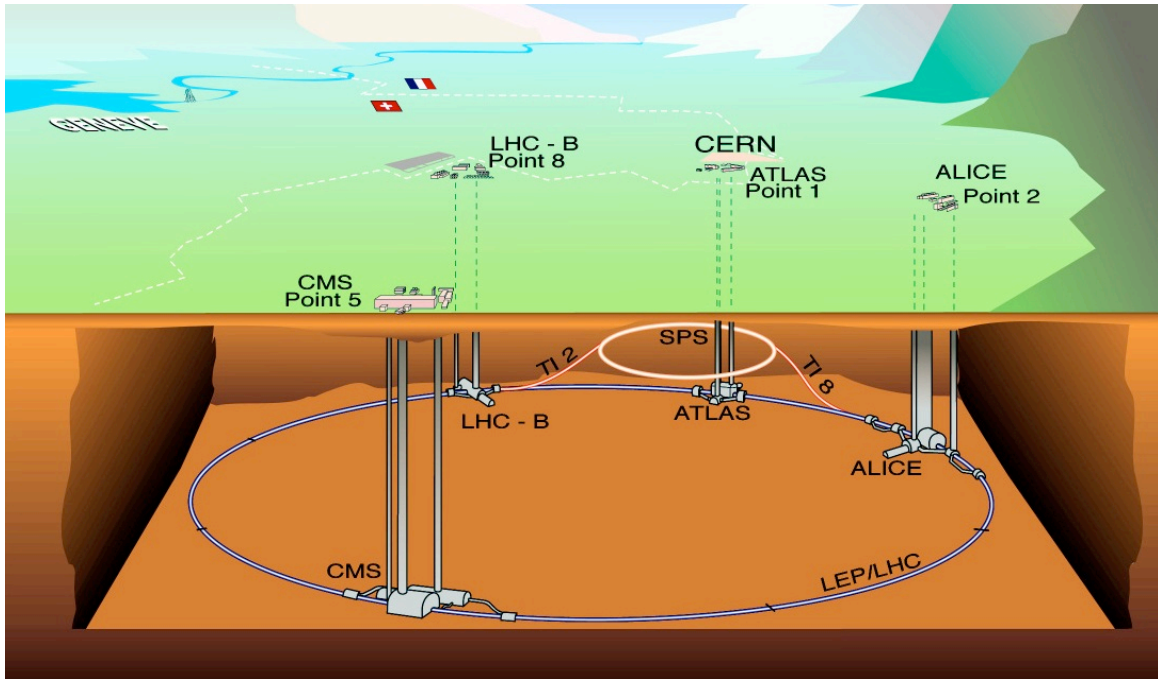
Figure 1: Map that shows the location of the LHC in relation to the Swiss/France border.[2]
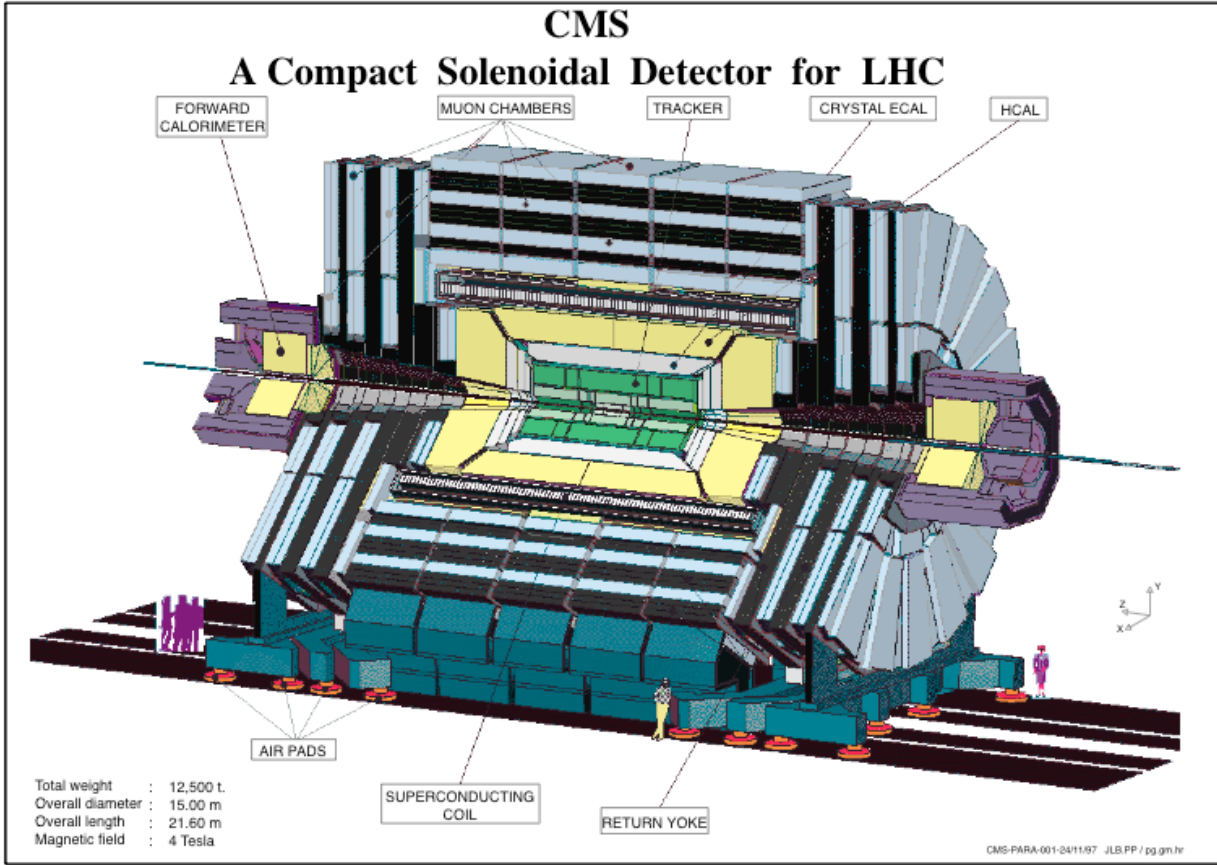
Figure 2: Diagram of the CMS detector.[3]
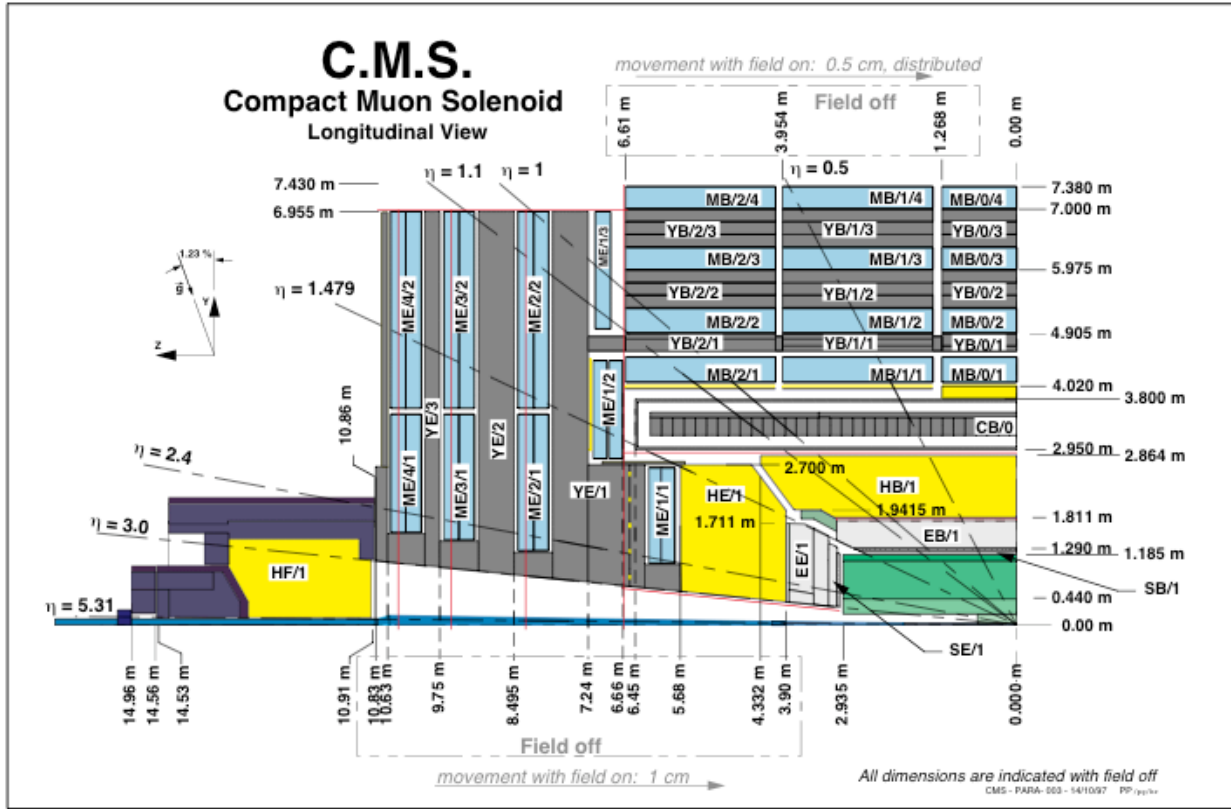
Figure 3: Diagram of the CMS detector.[3]
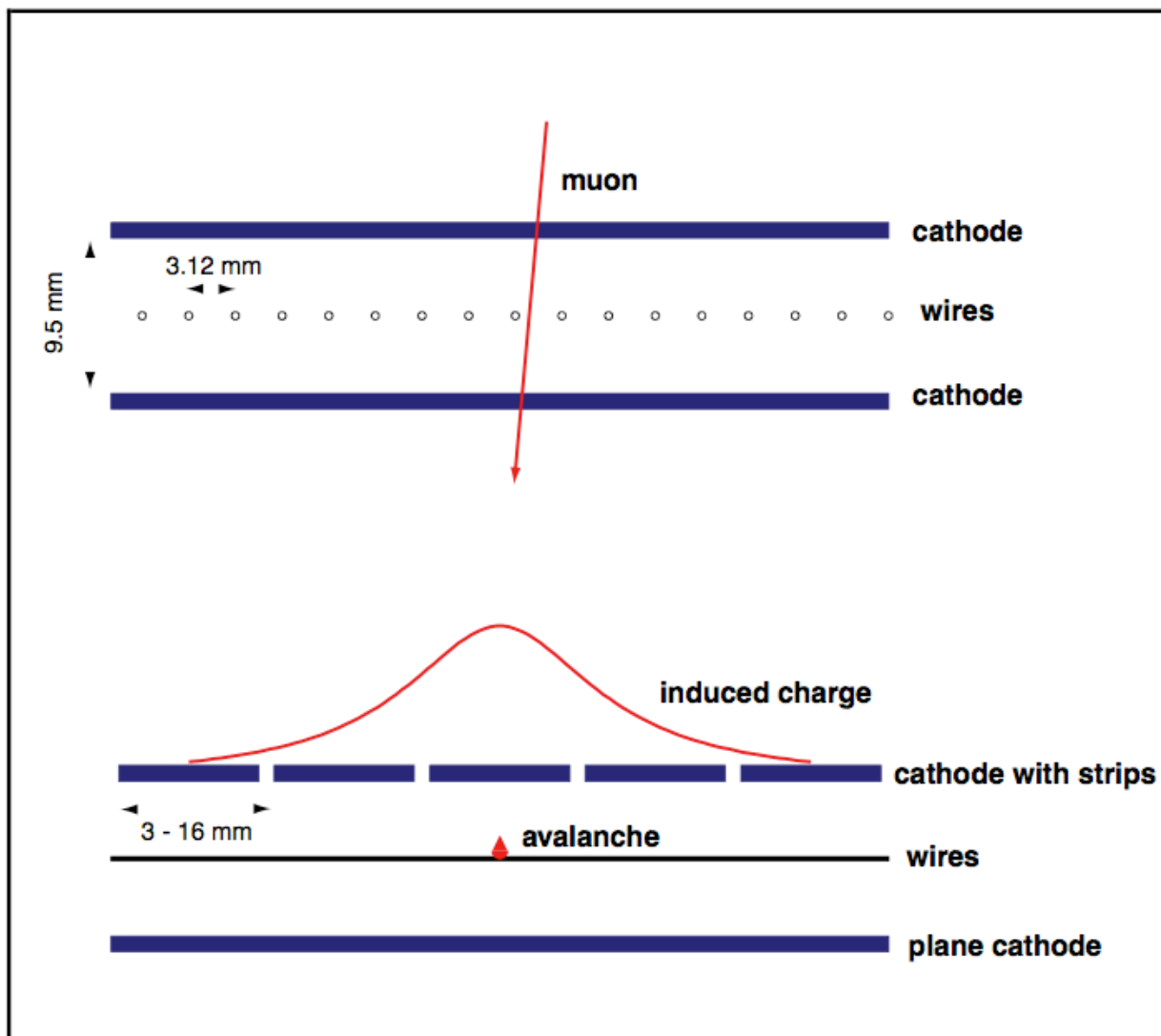
Figure 4: Diagram of a muon passing through a layer of a CSC. The muon induces a charge on both the anode wire and the cathode strip that is used to obtain a spatial measurement in two dimensions.[3]

Number of Unpacker Tracks Per Event:

Entries	296958
Mean	0.3826
RMS	0.4996
Underflow	0
Overflow	0
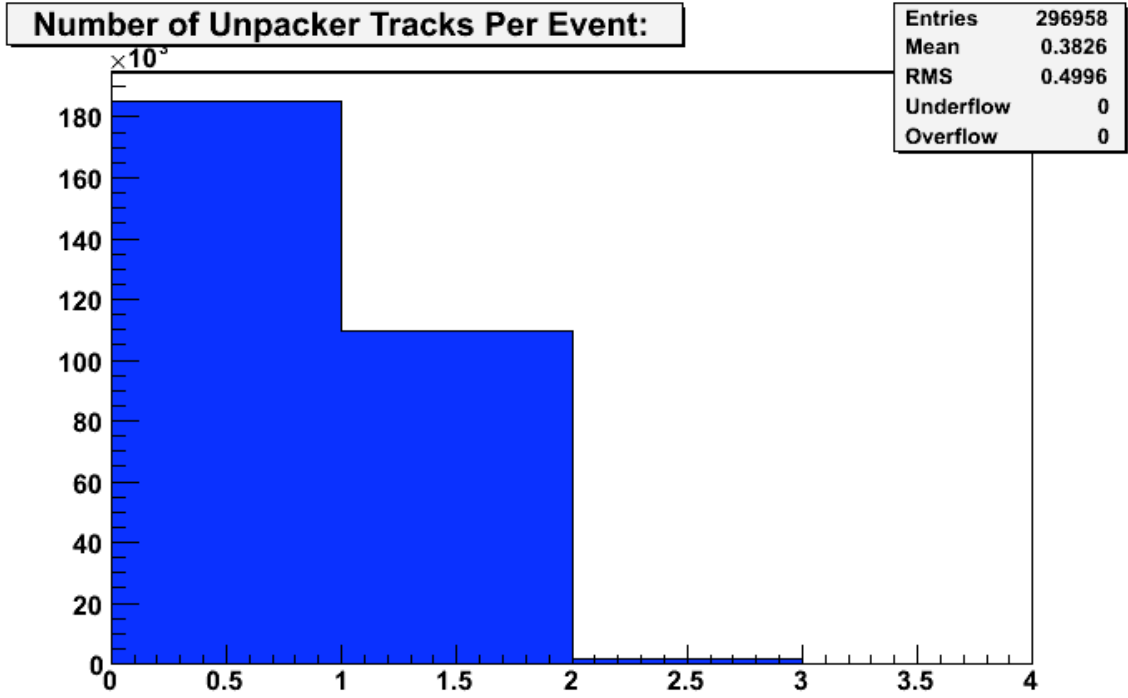
Figure 5: Number of tracks per event observed by the online CSC Track Finder.
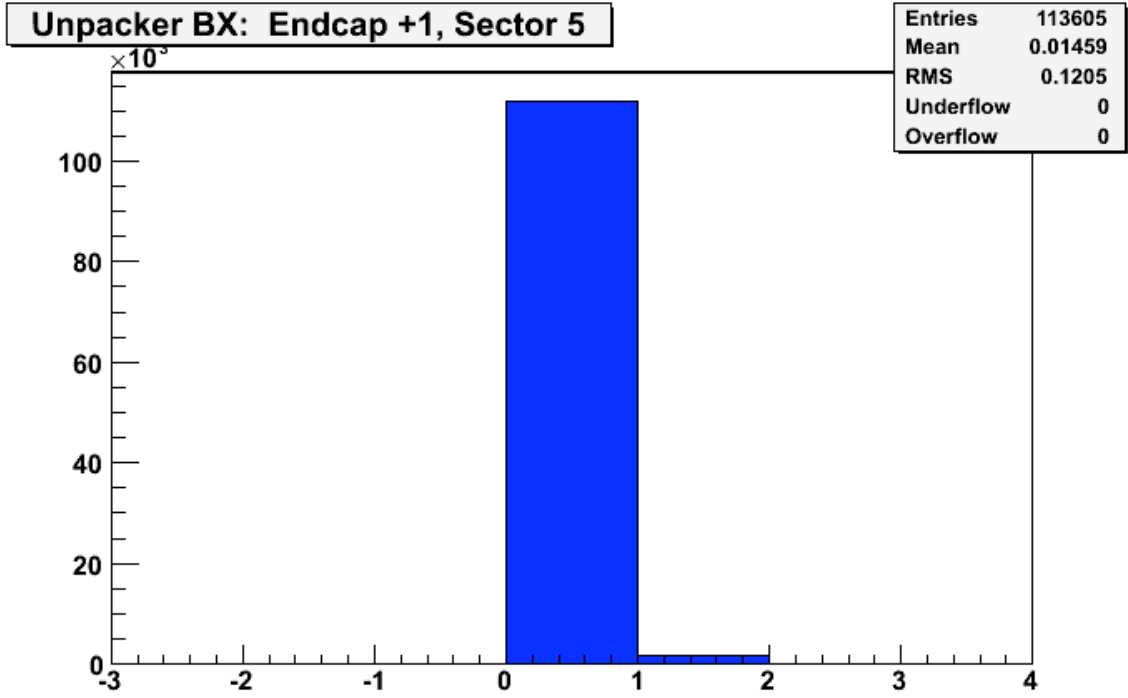
Figure 6: Relative timing of tracks found in the online CSC Track Finder in units of bunch crossings.
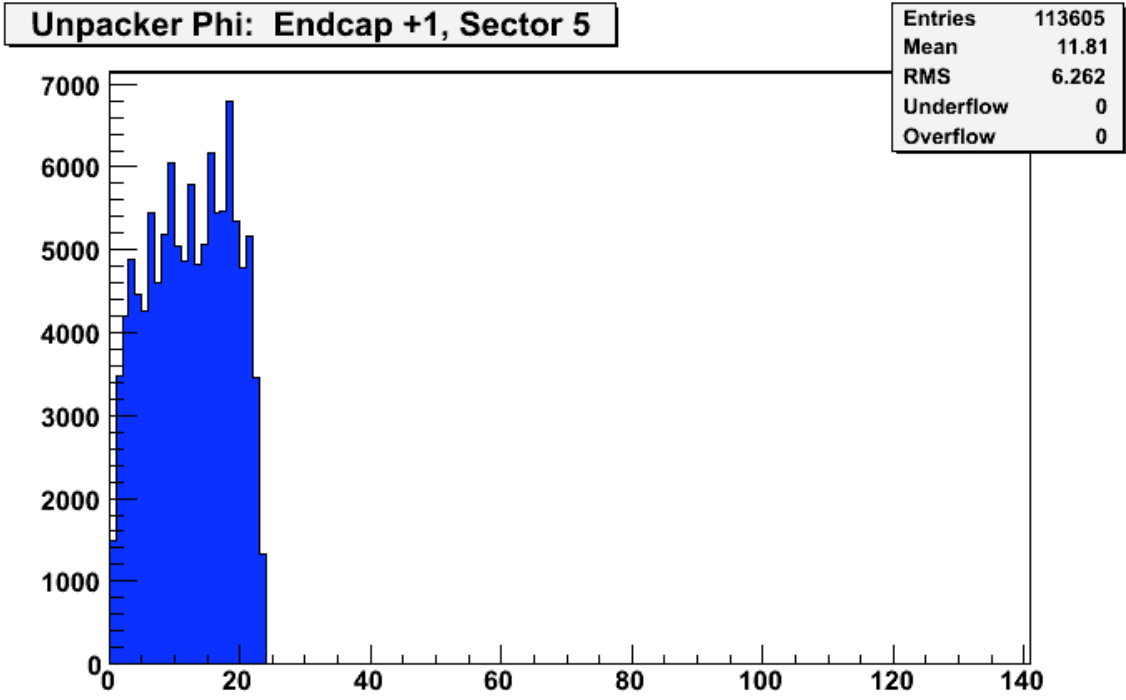
Figure 7: ϕ position assigned to tracks observed in the online CSC Track Finder.
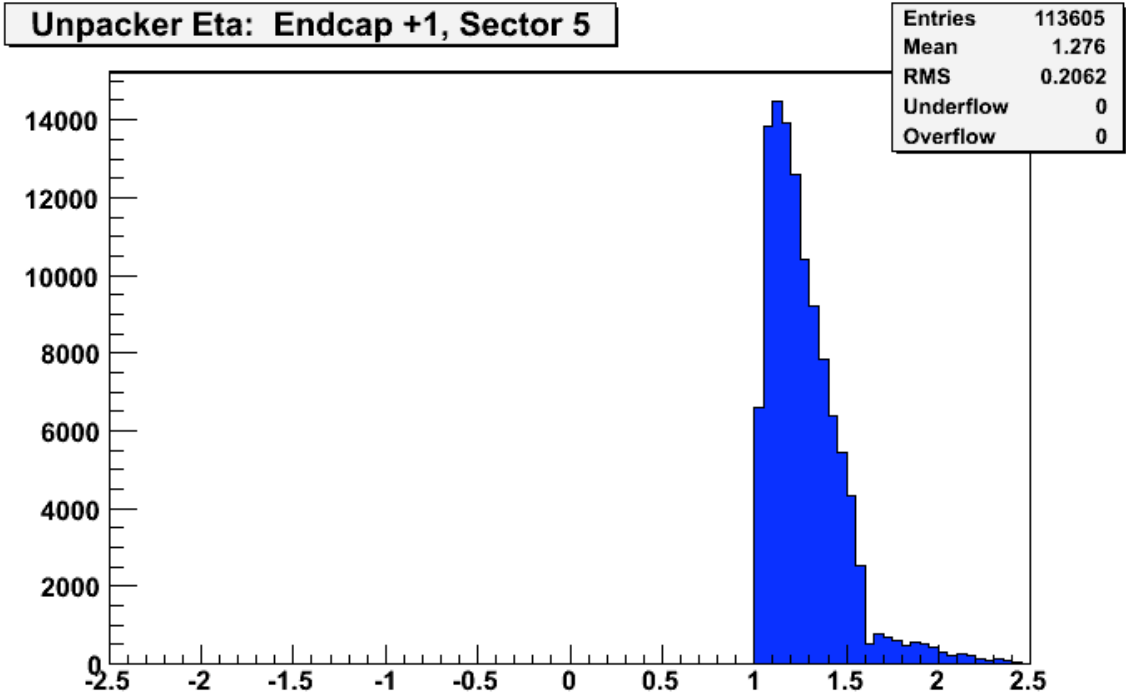
Figure 8: η position assigned to tracks observed in the online CSC Track Finder.
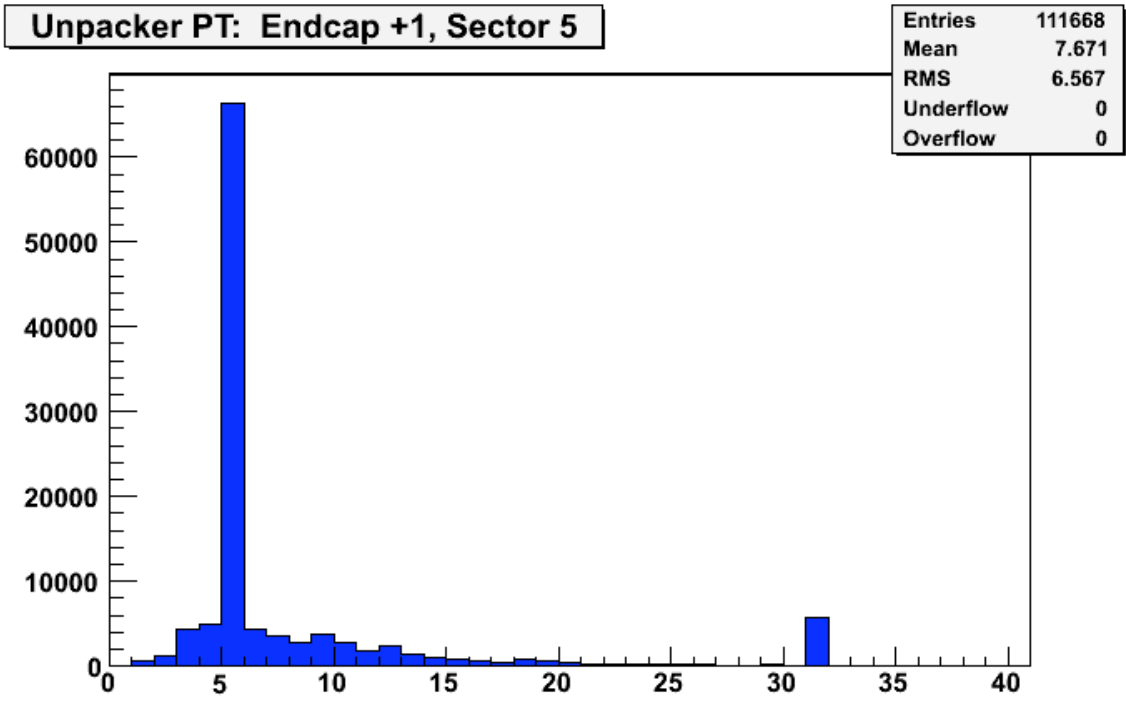
Figure 9: P$_T$ value assigned to tracks observed in the online CSC Track Finder.
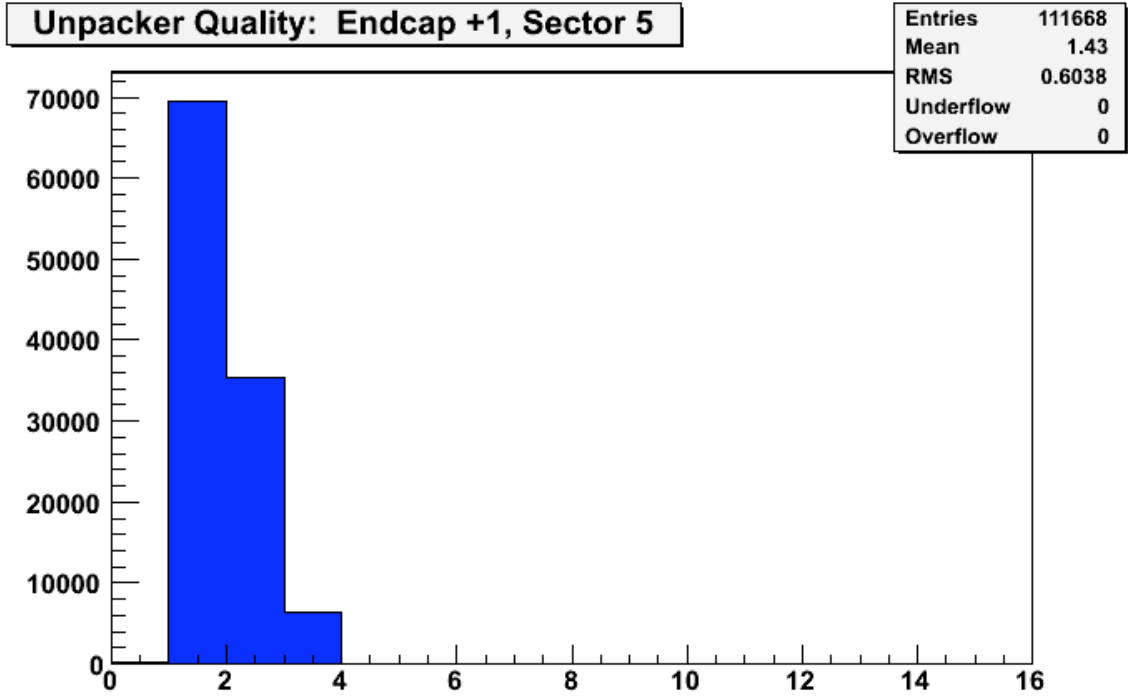
Figure 10: Quality assigned to tracks observed in the online CSC Track Finder.
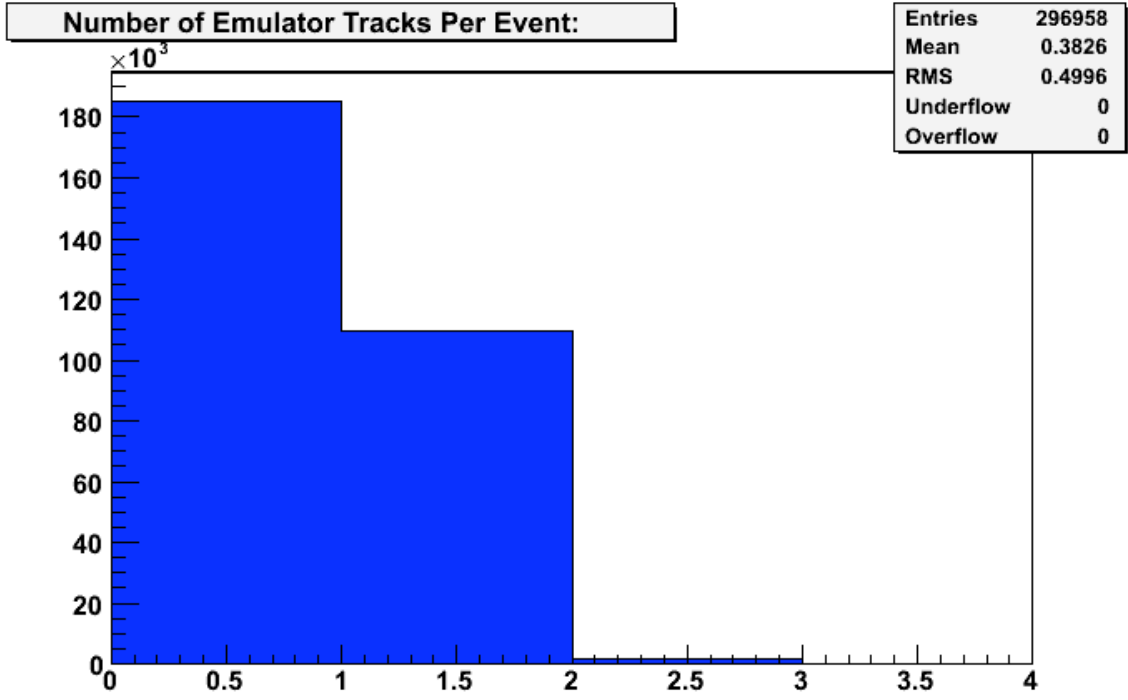
Figure 11: Number of tracks per event observed by the Track Finder Emulator.
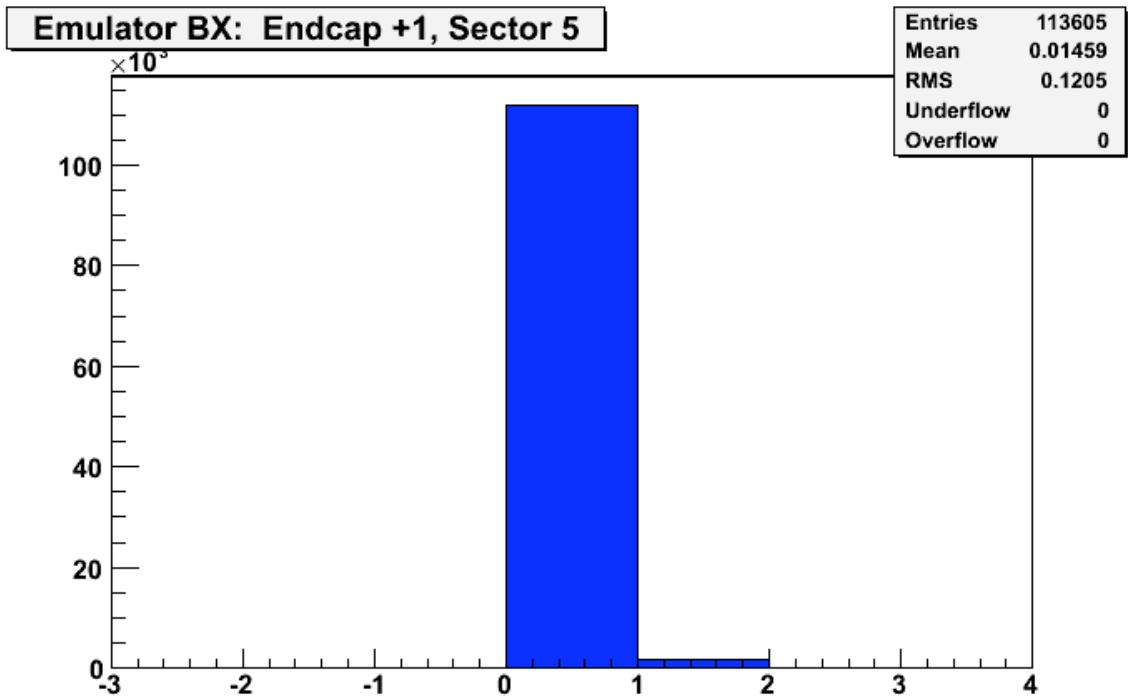
Figure 12: Relative timing of tracks found in the Track Finder Emulator in units of bunch crossings.
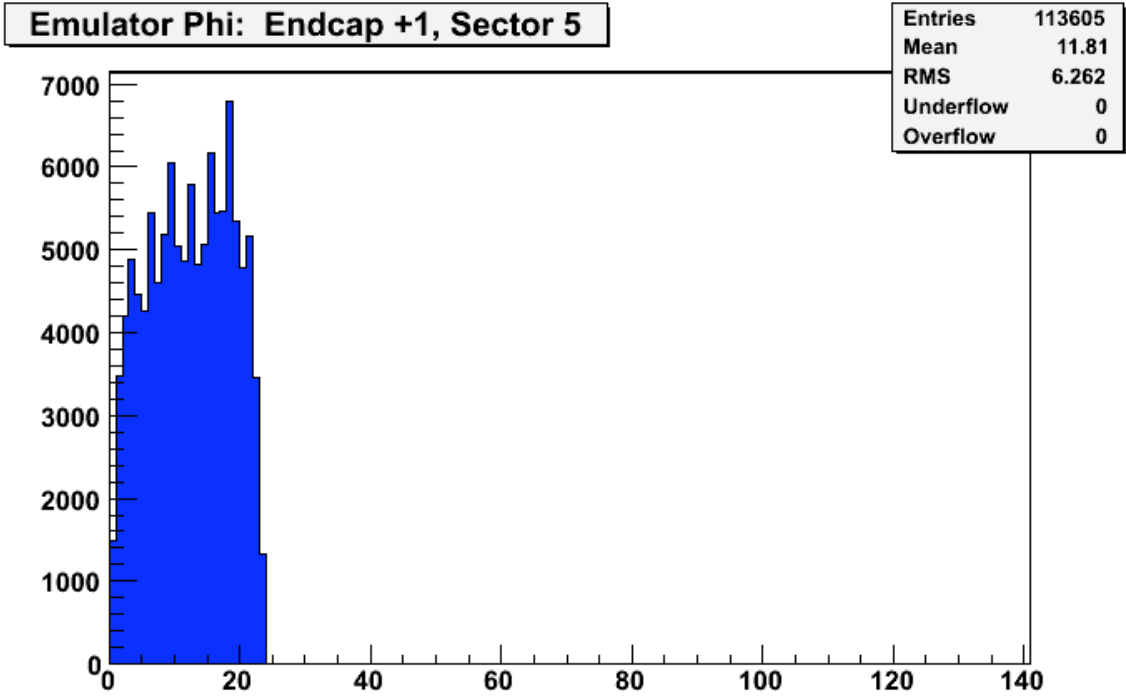
Figure 13: ϕ position assigned to tracks observed in the Track Finder Emulator.
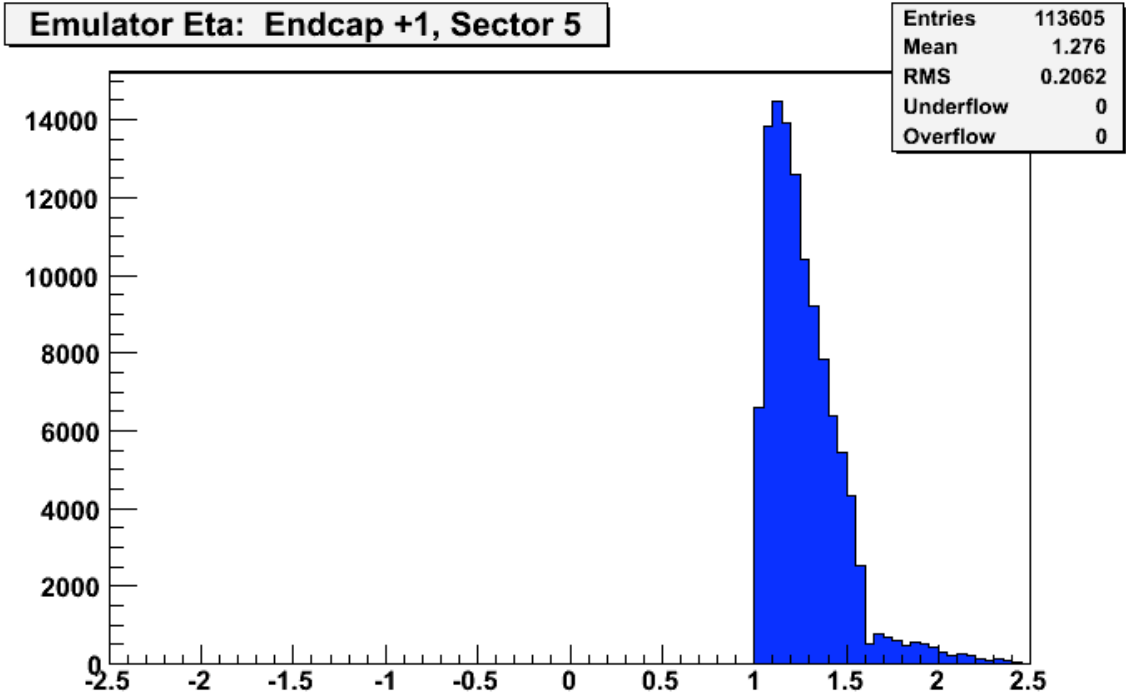
Figure 14: η position assigned to tracks observed in the Track Finder Emulator.
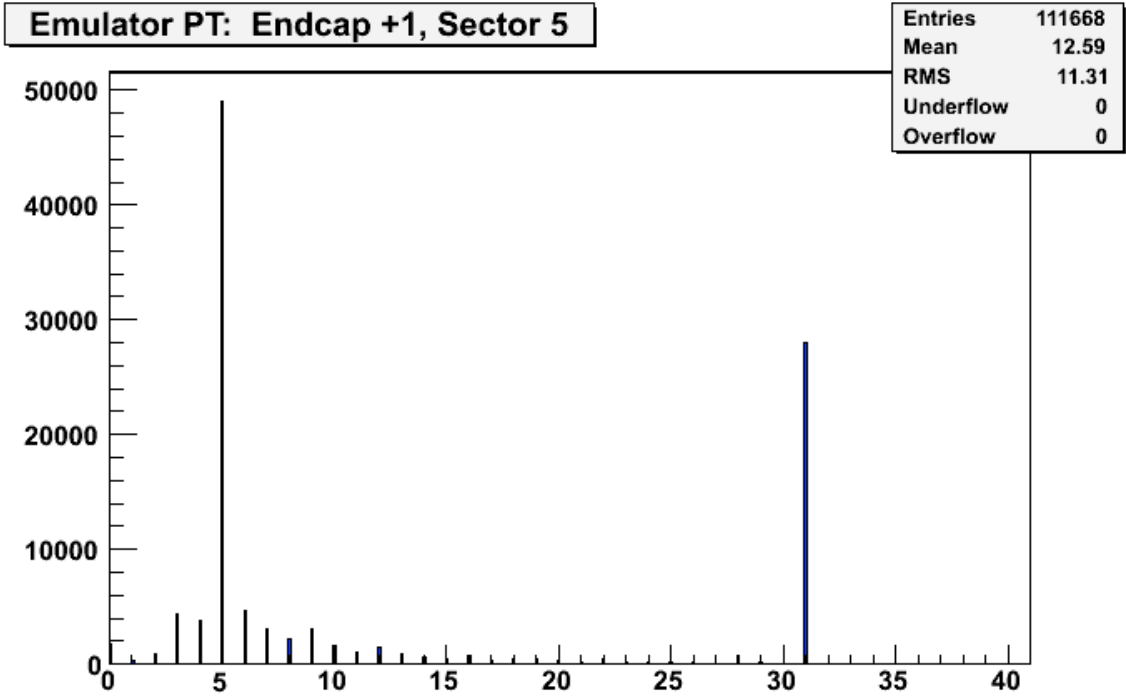
Figure 15: P$_T$ value assigned to tracks observed in the Track Finder Emulator.
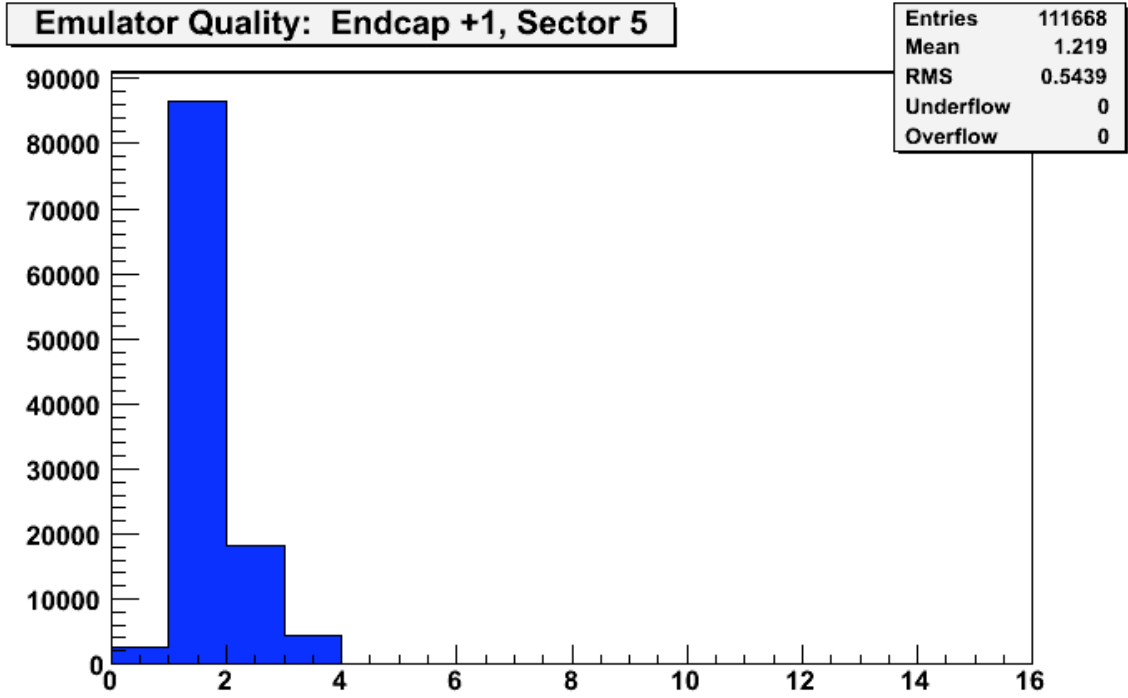
Figure 16: Quality assigned to tracks observed in the Track Finder Emulator.
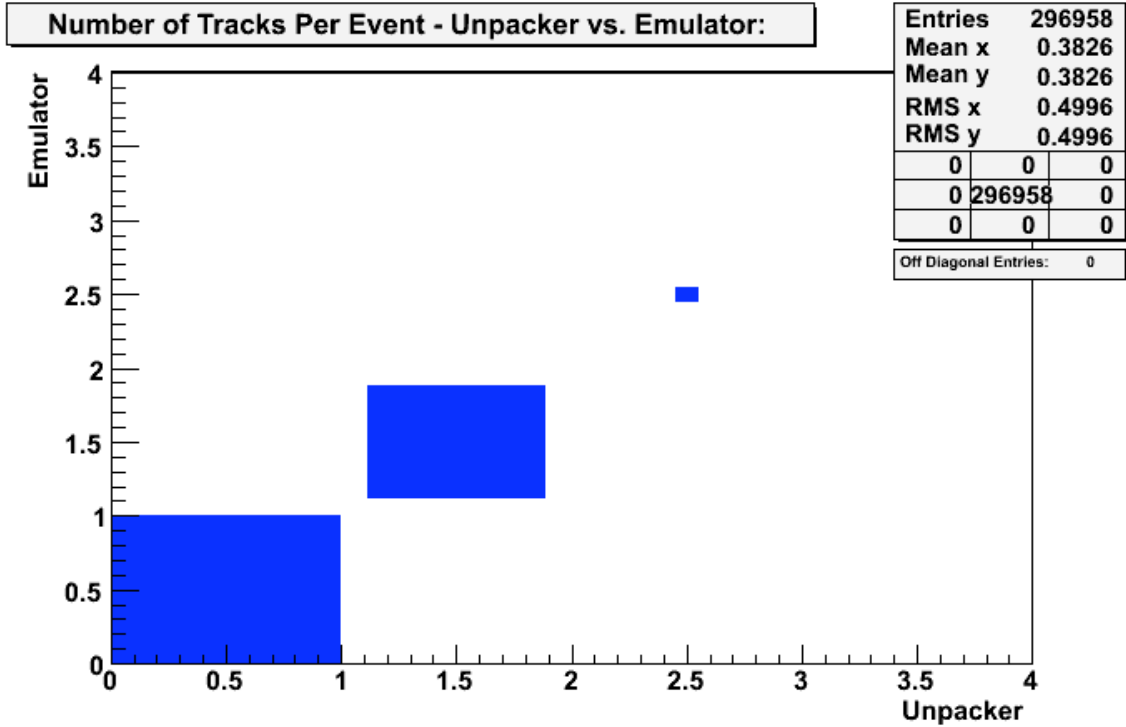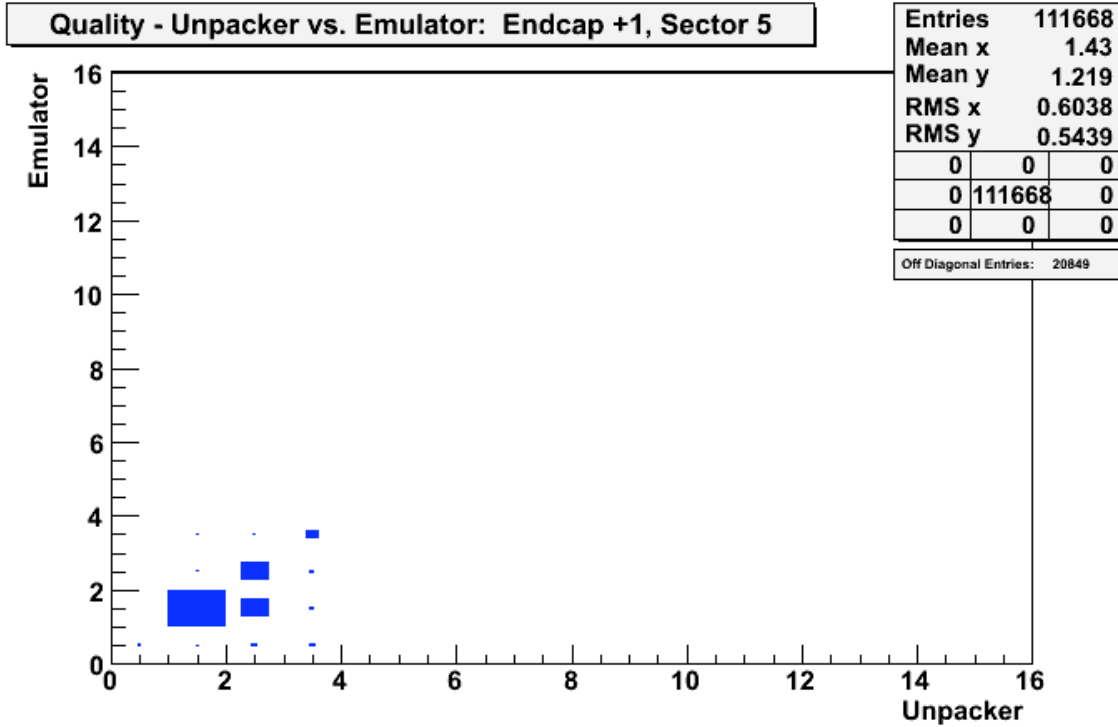
Figure 17: A comparison of the number of tracks found per event in the online CSC Track Finder (X-Axis) and the Track Finder Emulator (Y-Axis). The relative size of the boxes is proportional to the number of counts in that bin. Any disagreement in the number of tracks found would appear as an entry off the diagonal line.
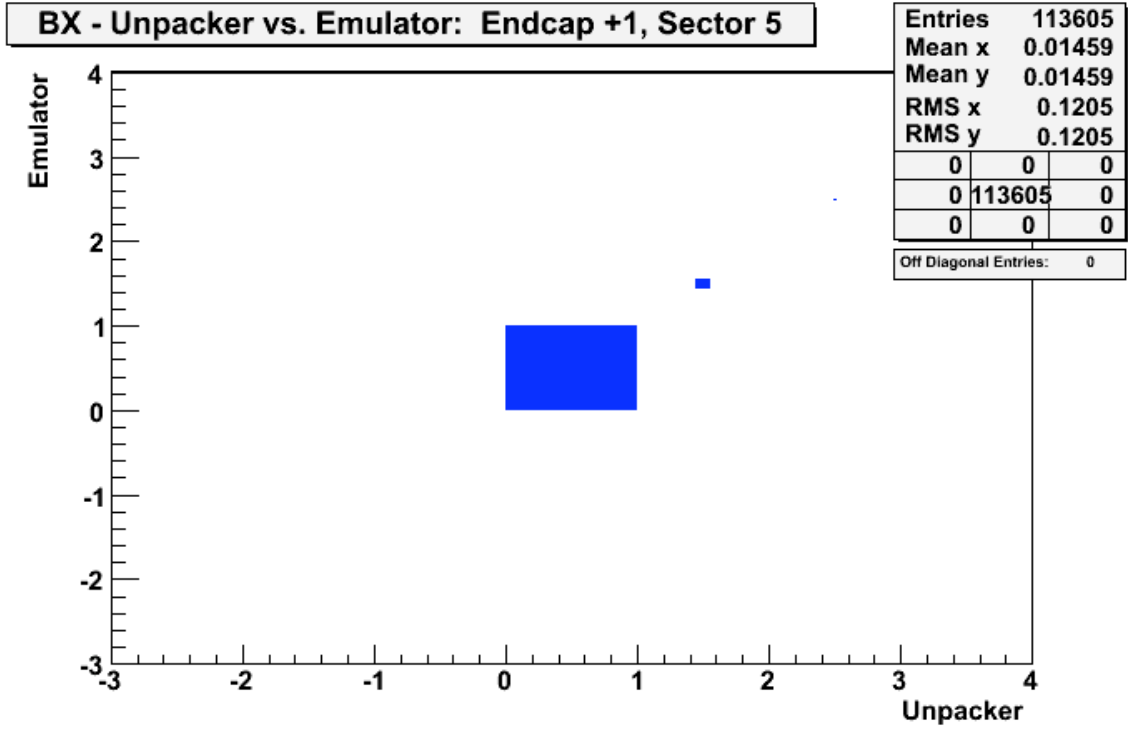
Figure 18: A comparison of the relative timing for tracks found per event in the online CSC Track Finder (X-Axis) and the Track Finder Emulator (Y-Axis). The relative size of the boxes is proportional to the number of counts in that bin. Any disagreement in the relative timing would appear as an entry off the diagonal line.

Phi - Unpacker vs. Emulator: Endcap +1, Sector 5

Entries	113605
Mean x	11.81
Mean y	11.81
RMS x	6.262
RMS y	6.262

0	0	0
0	113605	0
0	0	0

Off Diagonal Entries: 0
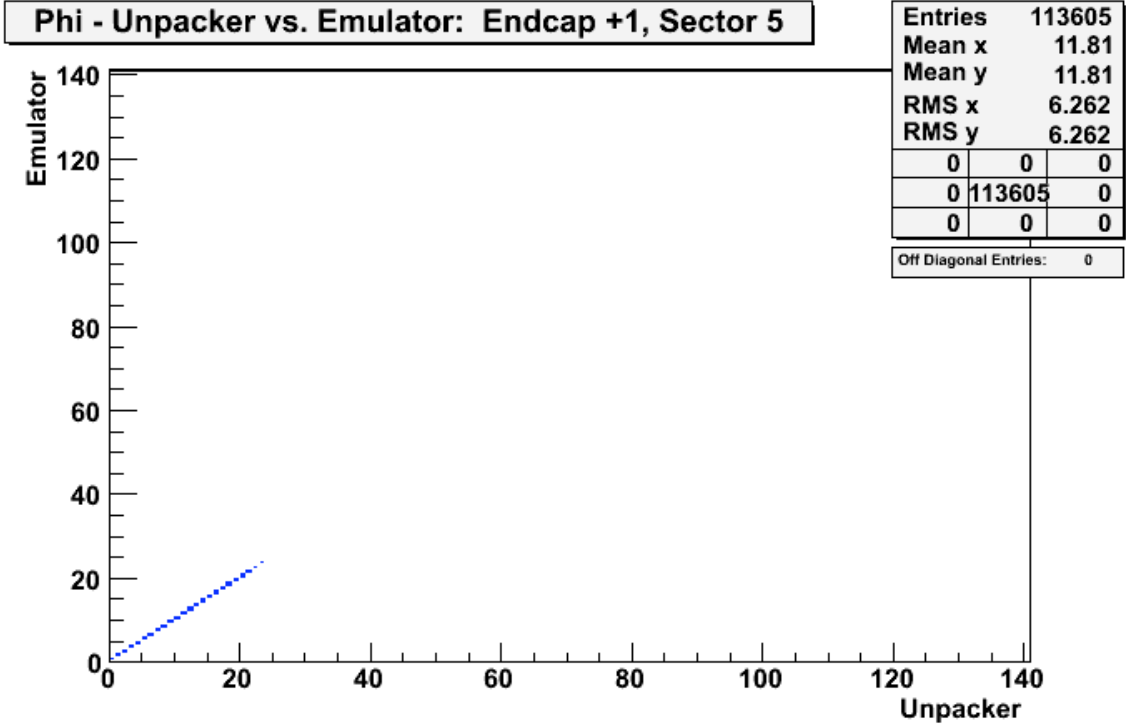
Figure 19: A comparison of the value of ϕ for tracks found per event in the online CSC Track Finder (X-Axis) and the Track Finder Emulator (Y-Axis). The relative size of the boxes is proportional to the number of counts in that bin. Any disagreement in the ϕ value would appear as an entry off the diagonal line.
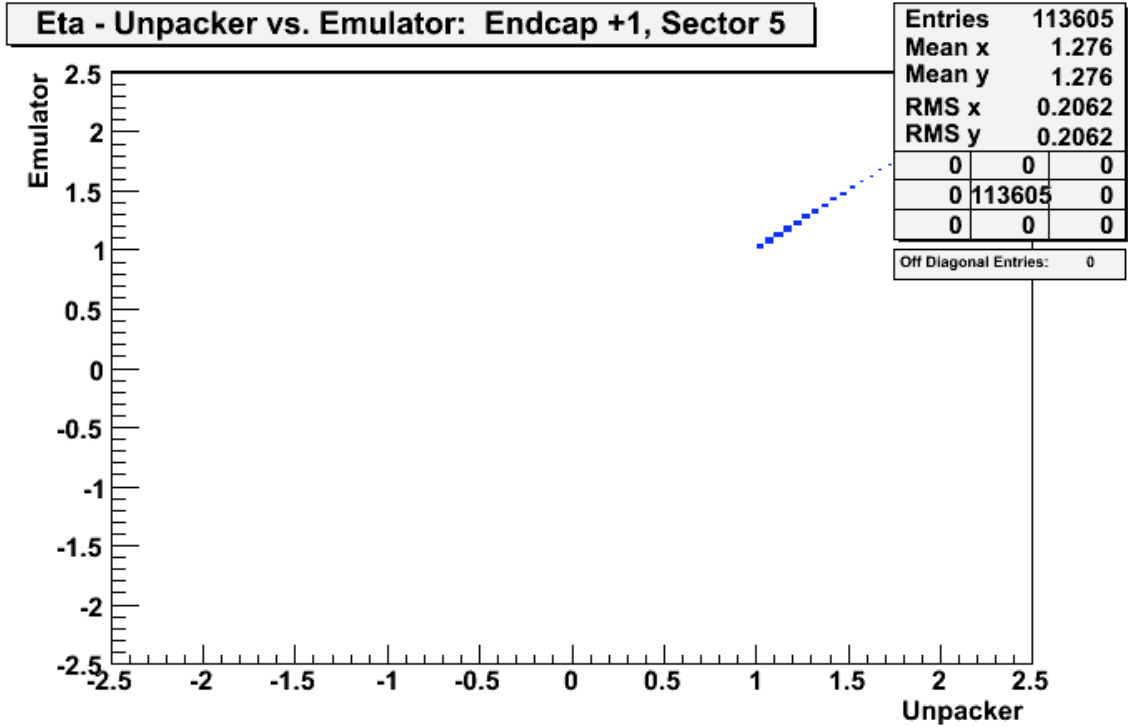
Figure 20: A comparison of the value of η for tracks found per event in the online CSC Track Finder (X-Axis) and the Track Finder Emulator (Y-Axis). The relative size of the boxes is proportional to the number of counts in that bin. Any disagreement in the η value would appear as an entry off the diagonal line.

PT - Unpacker vs. Emulator: Endcap +1, Sector 5

Entries		111668
Mean x		7.671
Mean y		12.59
RMS x		6.567
RMS y		11.31
0	0	0
0	111668	0
0	0	0

Off Diagonal Entries: 63231
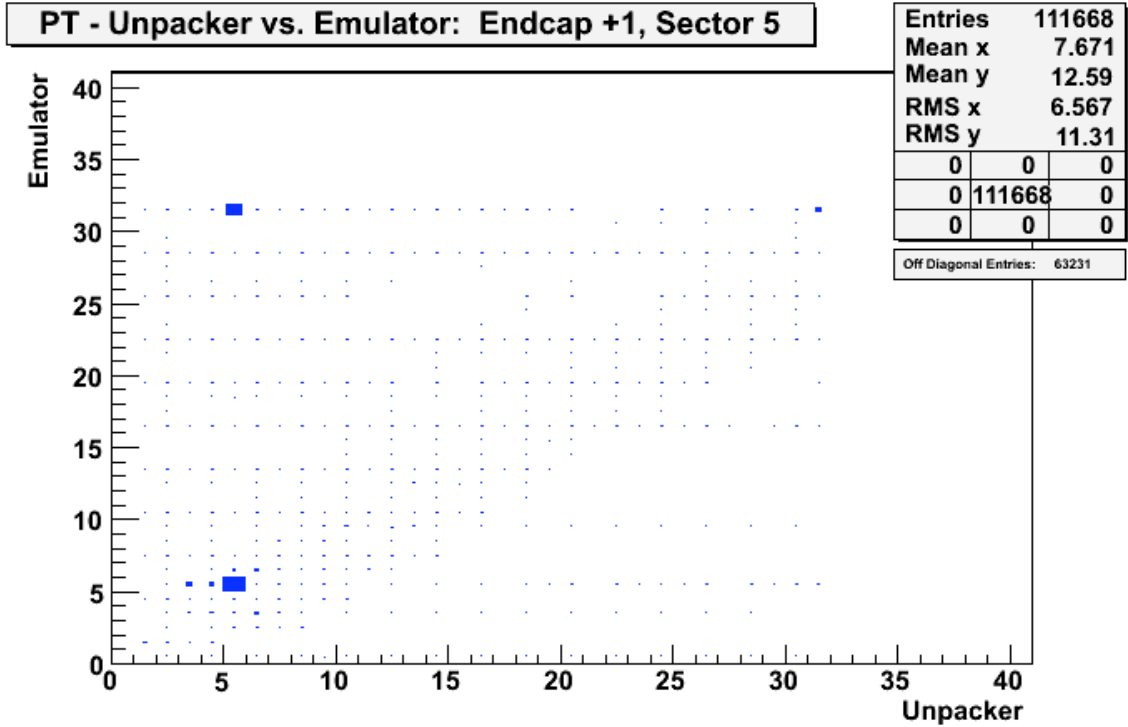
Figure 21: A comparison of the value of P_T for tracks found per event in the online CSC Track Finder (X-Axis) and the Track Finder Emulator (Y-Axis). The relative size of the boxes is proportional to the number of counts in that bin. Any disagreement in the assigned P_T would appear as an entry off the diagonal line.

Figure 22: A comparison of the value of quality for tracks found per event in the online CSC Track Finder (X-Axis) and the Track Finder Emulator (Y-Axis). The relative size of the boxes is proportional to the number of counts in that bin. Any disagreement in the assigned quality would appear as an entry off the diagonal line.
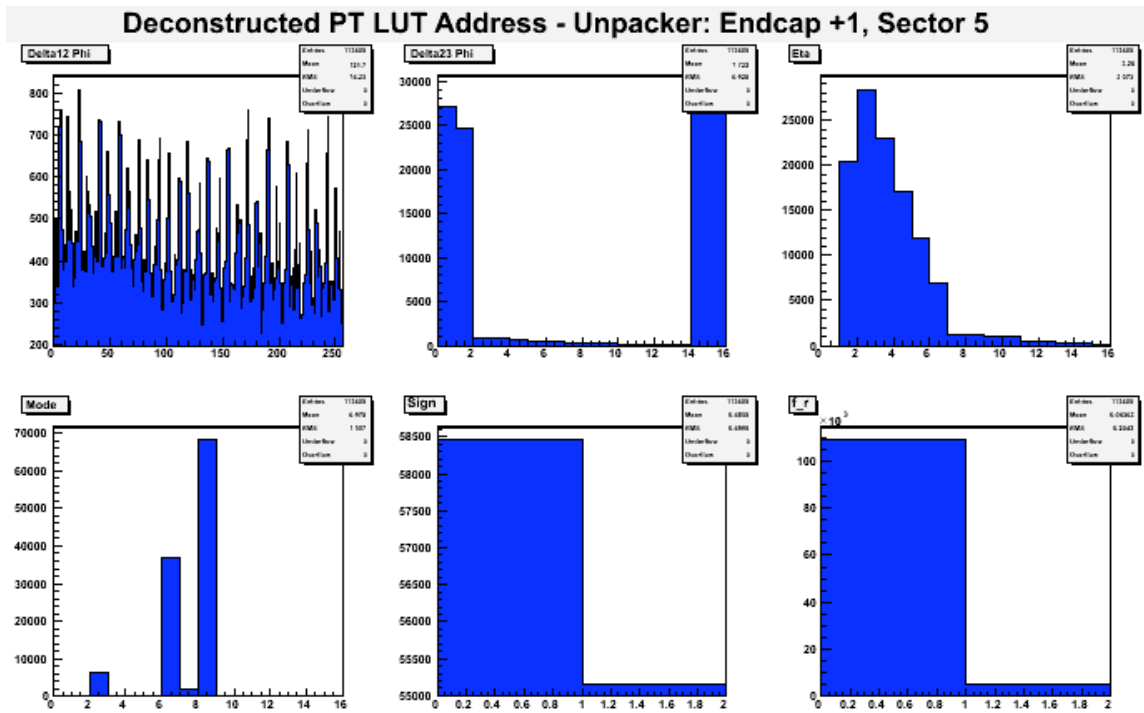
Figure 23: Deconstructed P_T LUT address assigned to tracks found by the online CSC Track Finder. Each of these plots show one of the words that make up the P_T LUT Address bit field.
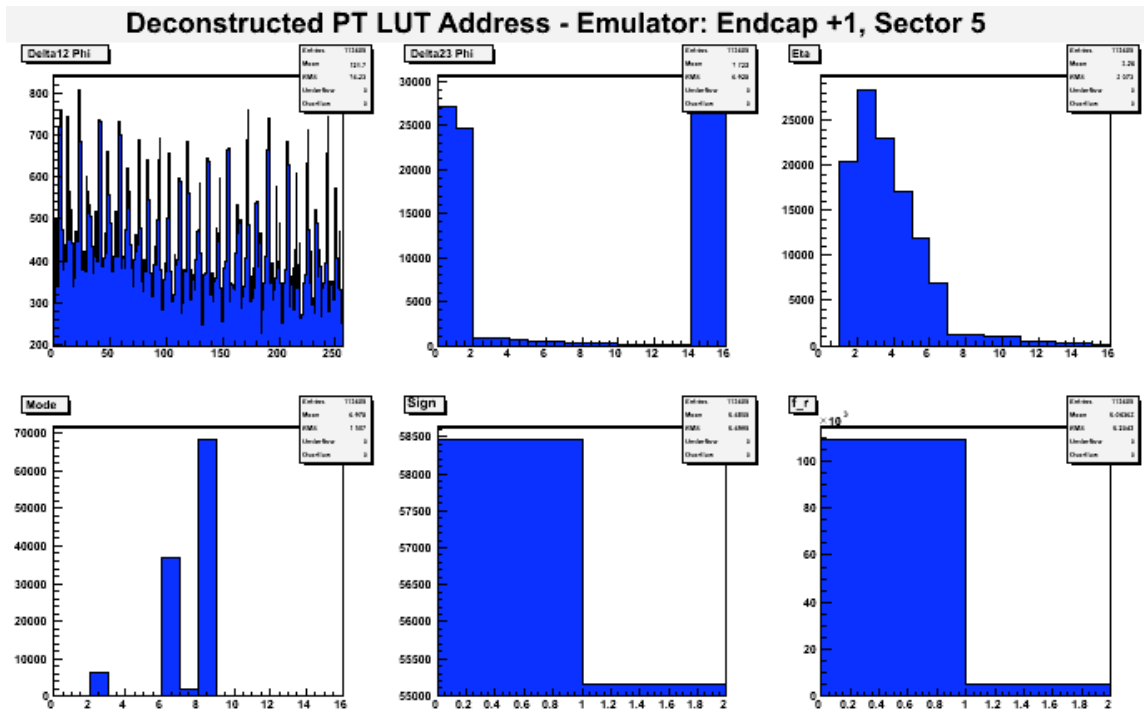
Figure 24: Deconstructed P_T LUT address assigned to tracks found by the Track Finder Emulator. Each of these plots show one of the words that make up the P_T LUT Address bit field.
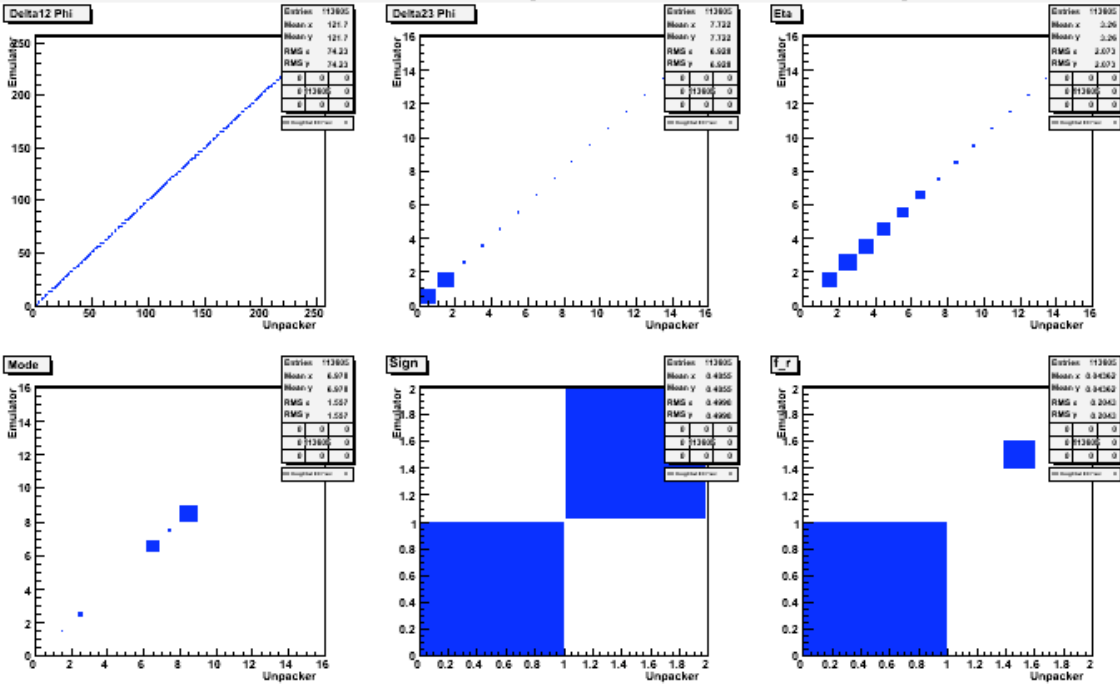
Figure 25: A comparison of the component words that make up the P_T LUT address for tracks found per event in the online CSC Track Finder (X-Axis) and the Track Finder Emulator (Y-Axis). The relative size of the boxes is proportional to the number of counts in that bin. Any disagreement in one of these data field would appear as an entry off the diagonal line.
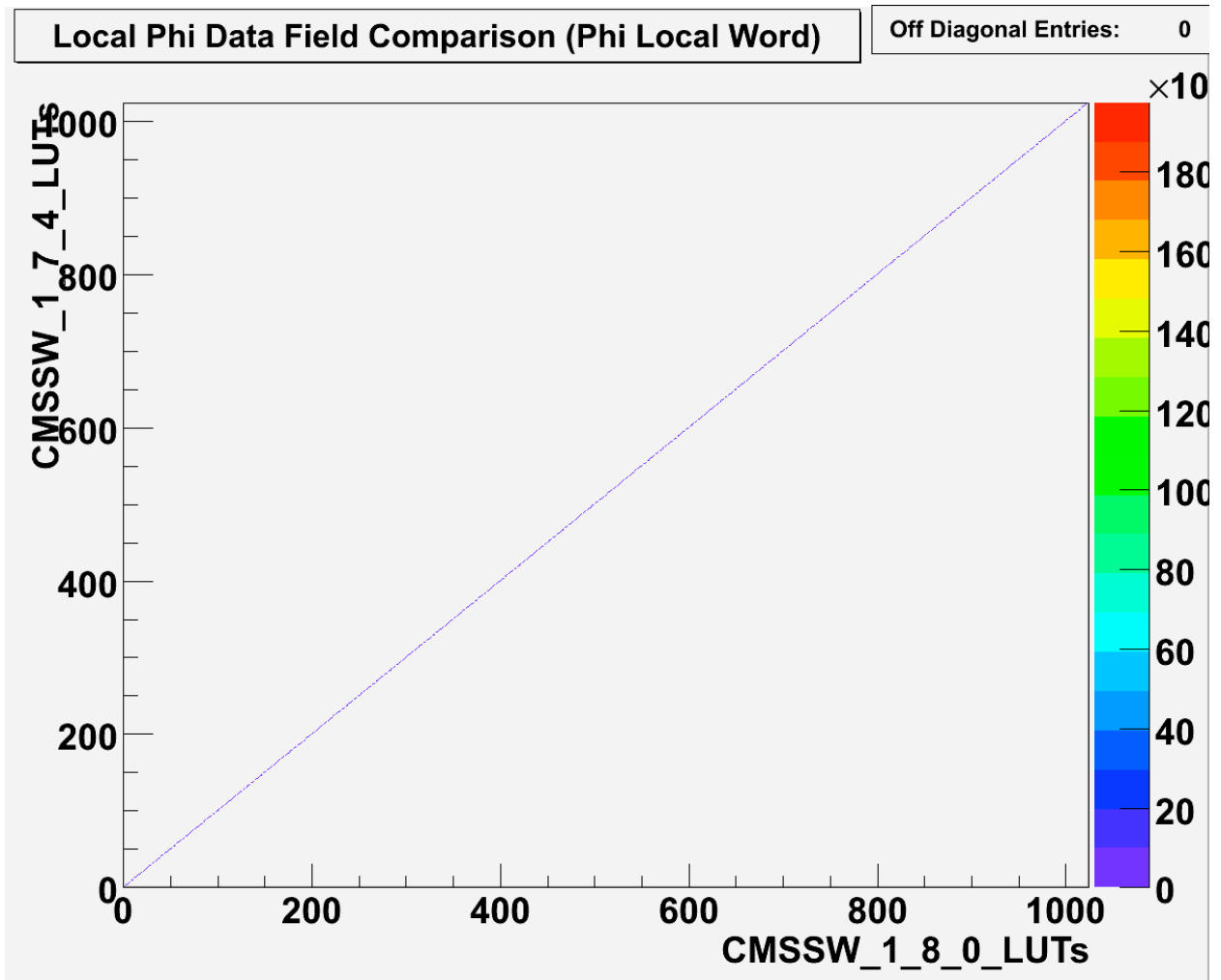
Figure 26: Comparison of the Local φ LUT. In this plot only the Phi Local word is compared because the Phi Bend Local word has not yet been implemented into the Local φ LUT. Mismatches in the data field would appear as entries off the diagonal line.
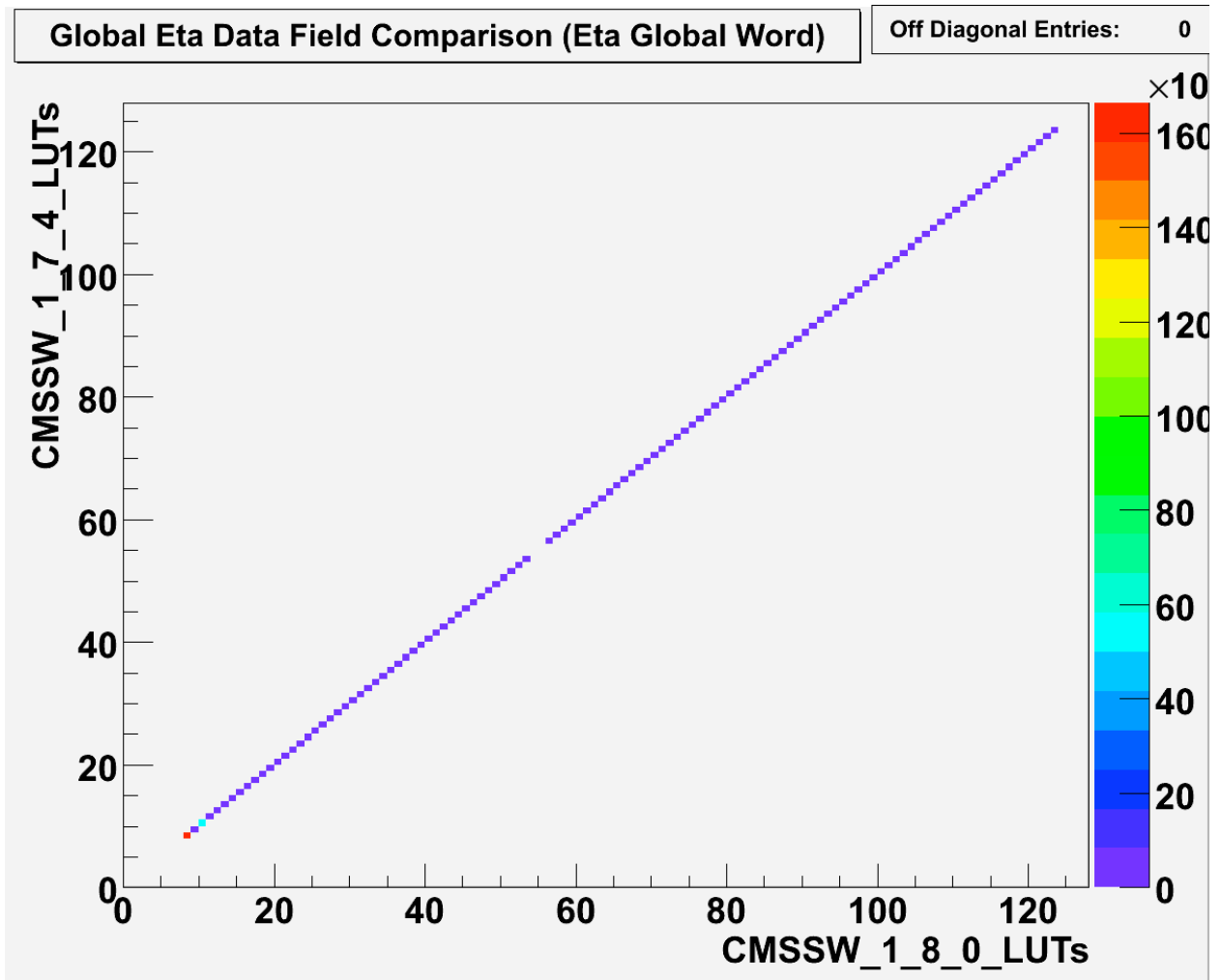
Figure 27: Comparison of the Global η LUT. In this plot only the Eta Global word is compared because the Phi Bend Global word has not yet been implemented into the Global η LUT. Also, only the LUT for endcap 1/sector 1/station 2 was compared. Mismatches in the data field would appear as entries off the diagonal line.
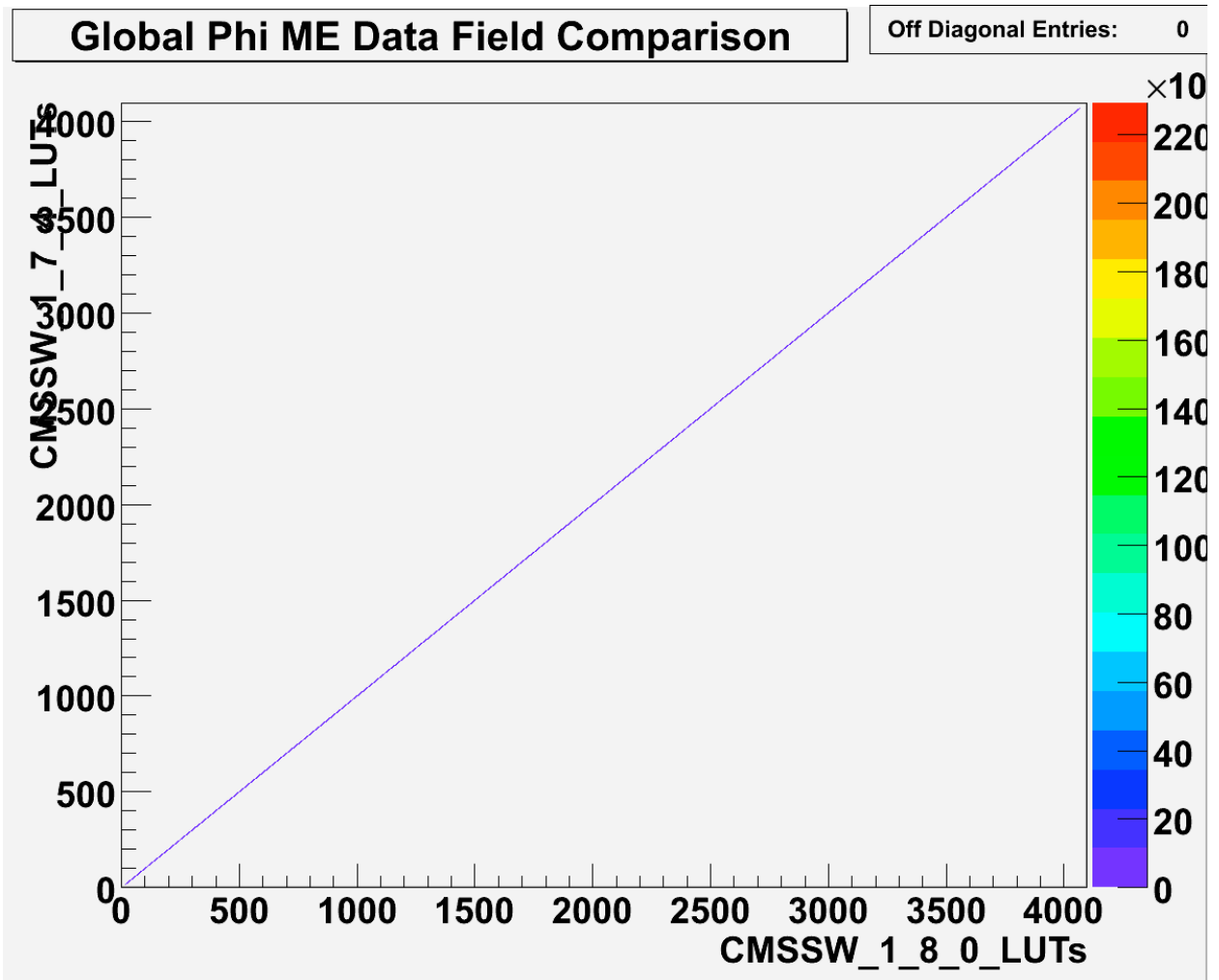
Figure 28: Comparison of the Global ϕ ME LUT. In this plots, only the LUT for endcap 1/sector 1/station 2 was compared. Mismatches in the data field would appear as entries off the diagonal line.
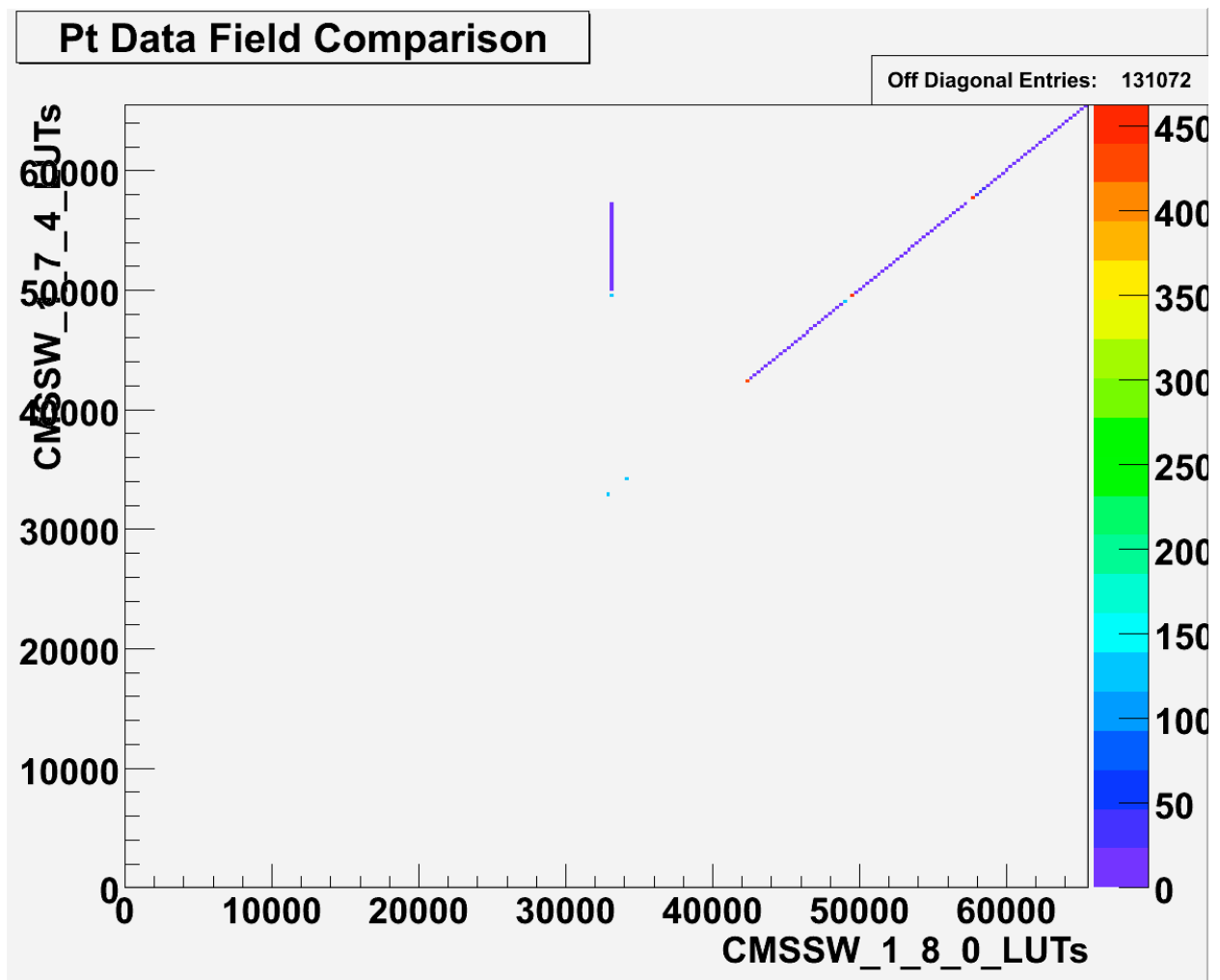
Figure 29: Comparison of the P_T LUT. Mismatches in the data field appear as entries off the diagonal line.
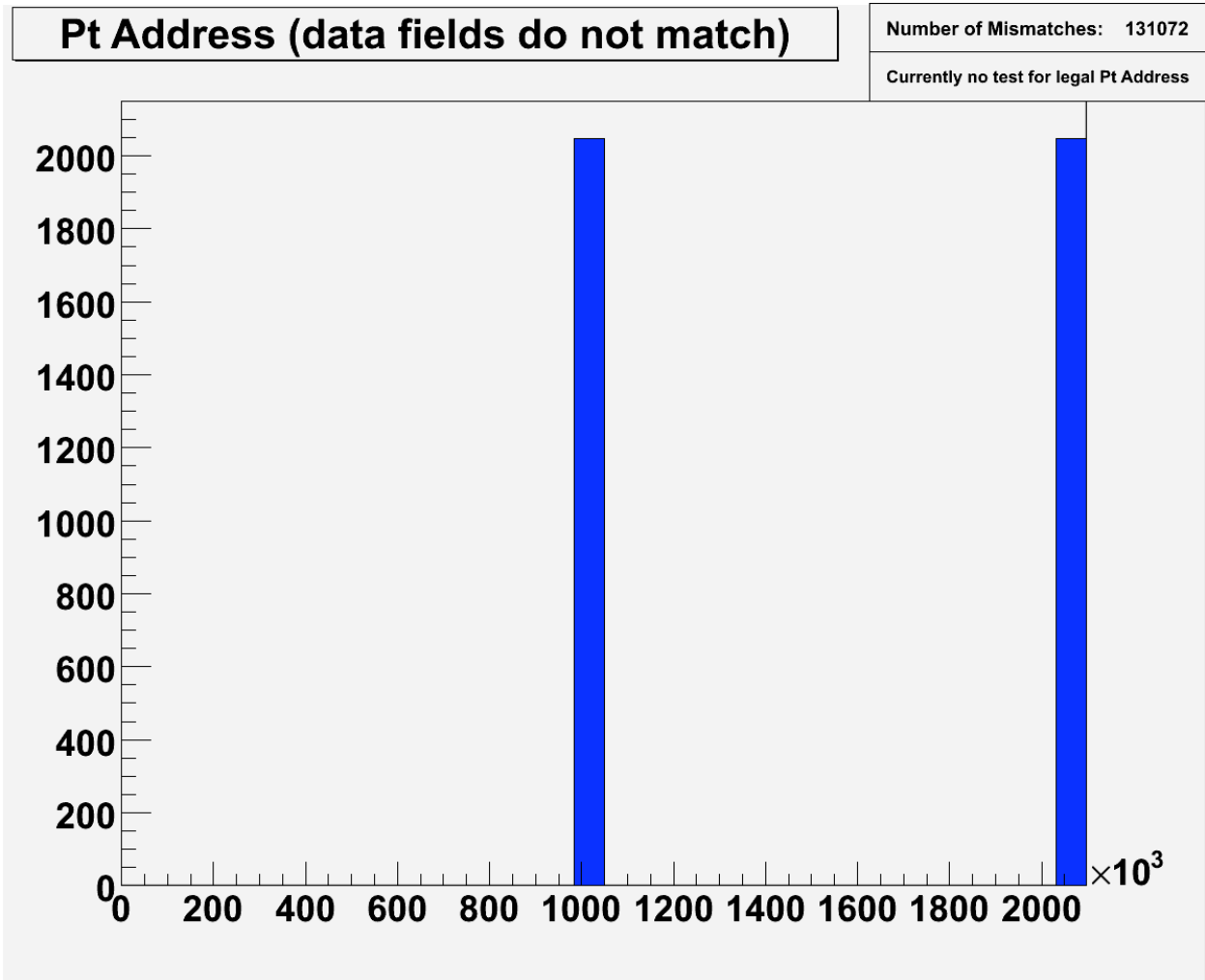
Figure 30: The P_T LUT address that contribute to the mismatches in P_T LUT data field seen in figure 29.
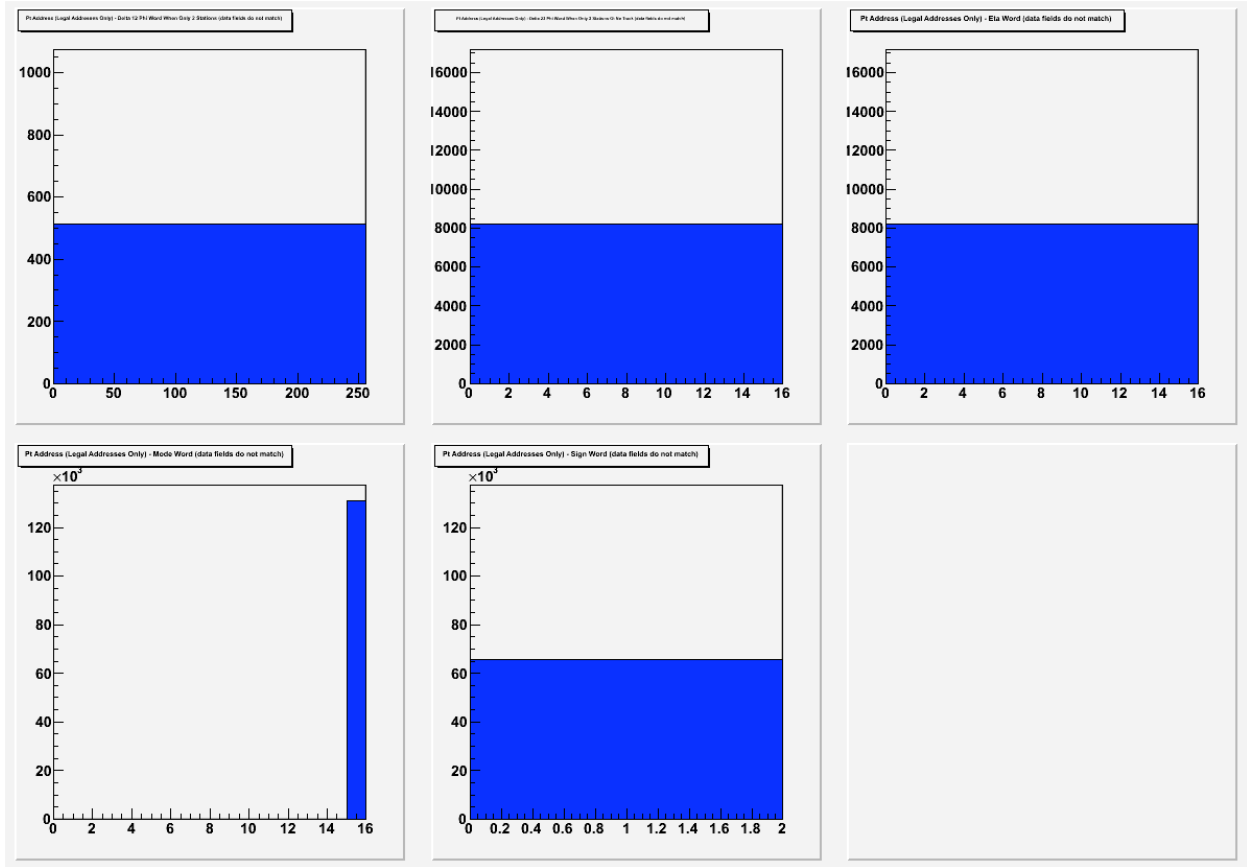
Figure 31: Component words of the P_T LUT address that contribute to the mismatches in P_T LUT data field seen in figure 29.

Global Phi (CSC) vs. Local Phi: Endcap 1, Sector 1, Station 1a, WG 1
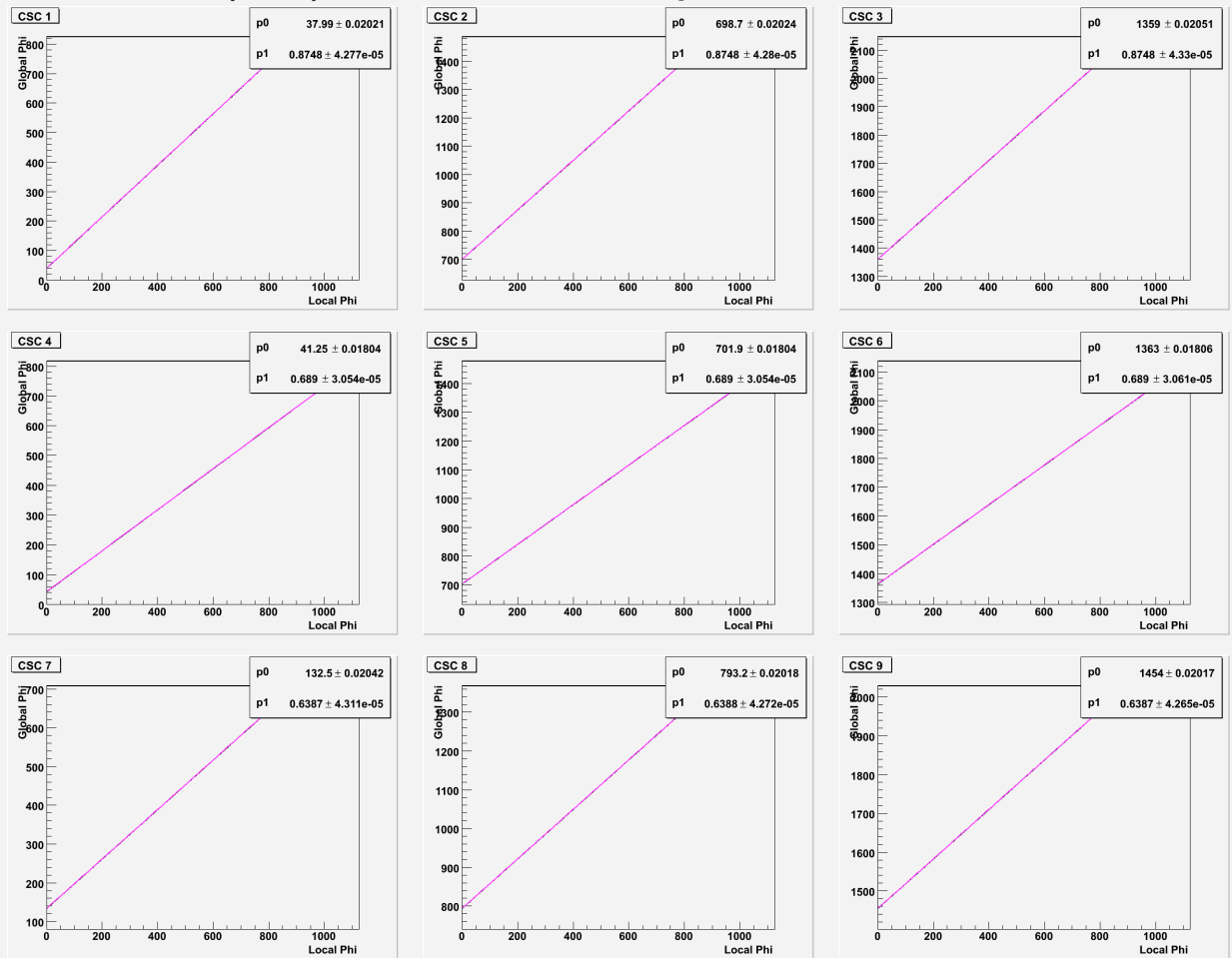
Figure 32: Global ϕ ME for CSCs in endcap 1/sector 1/station 1a. The magenta line overlaying the data points is the parameterized curve fit obtained by fitting equation 3 to these data.
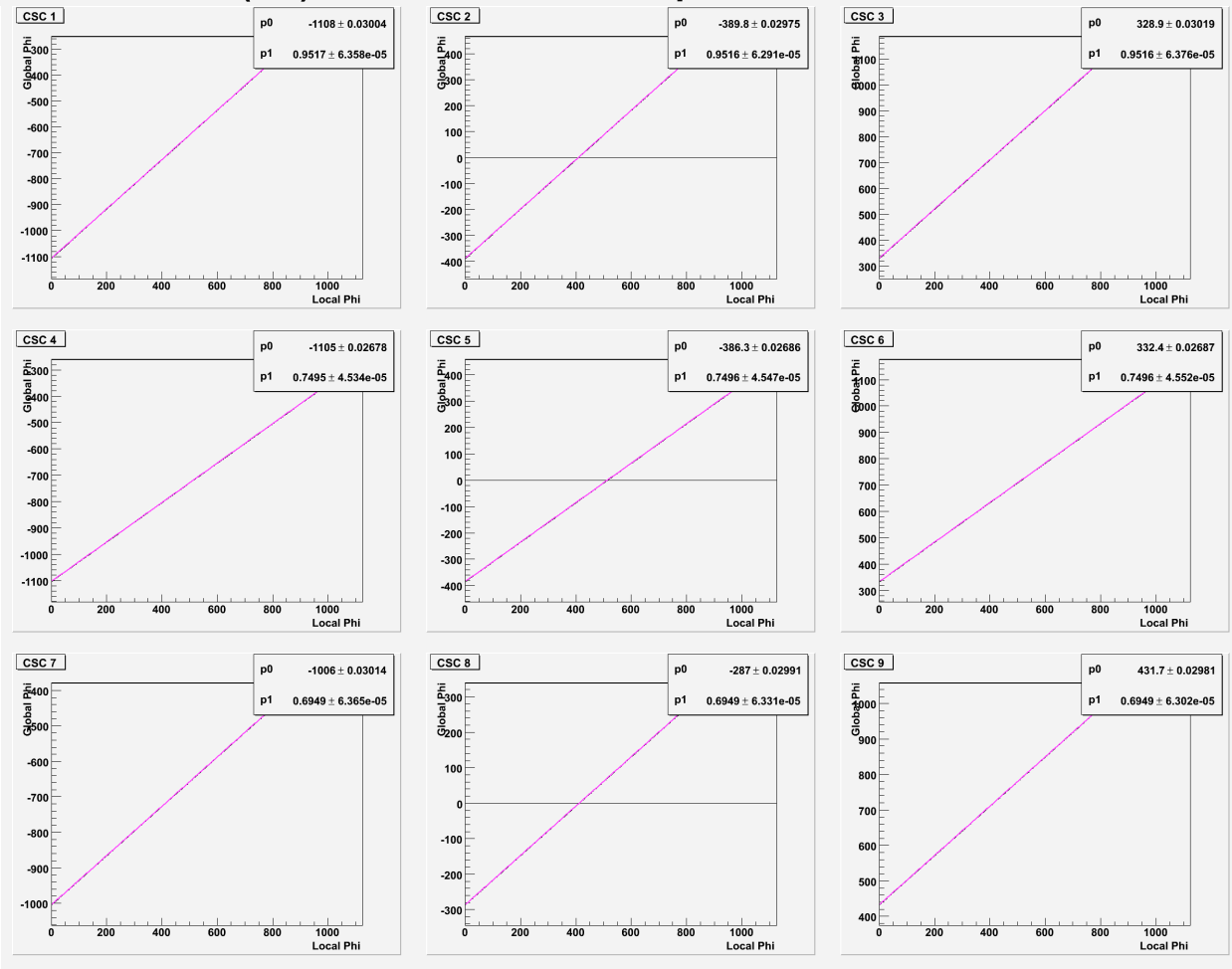
Figure 33: Global ϕ MB for CSCs in endcap 1/sector 1/station 1a. The magenta line overlaying the data points is the parameterized curve fit obtained by fitting equation 3 to these data.
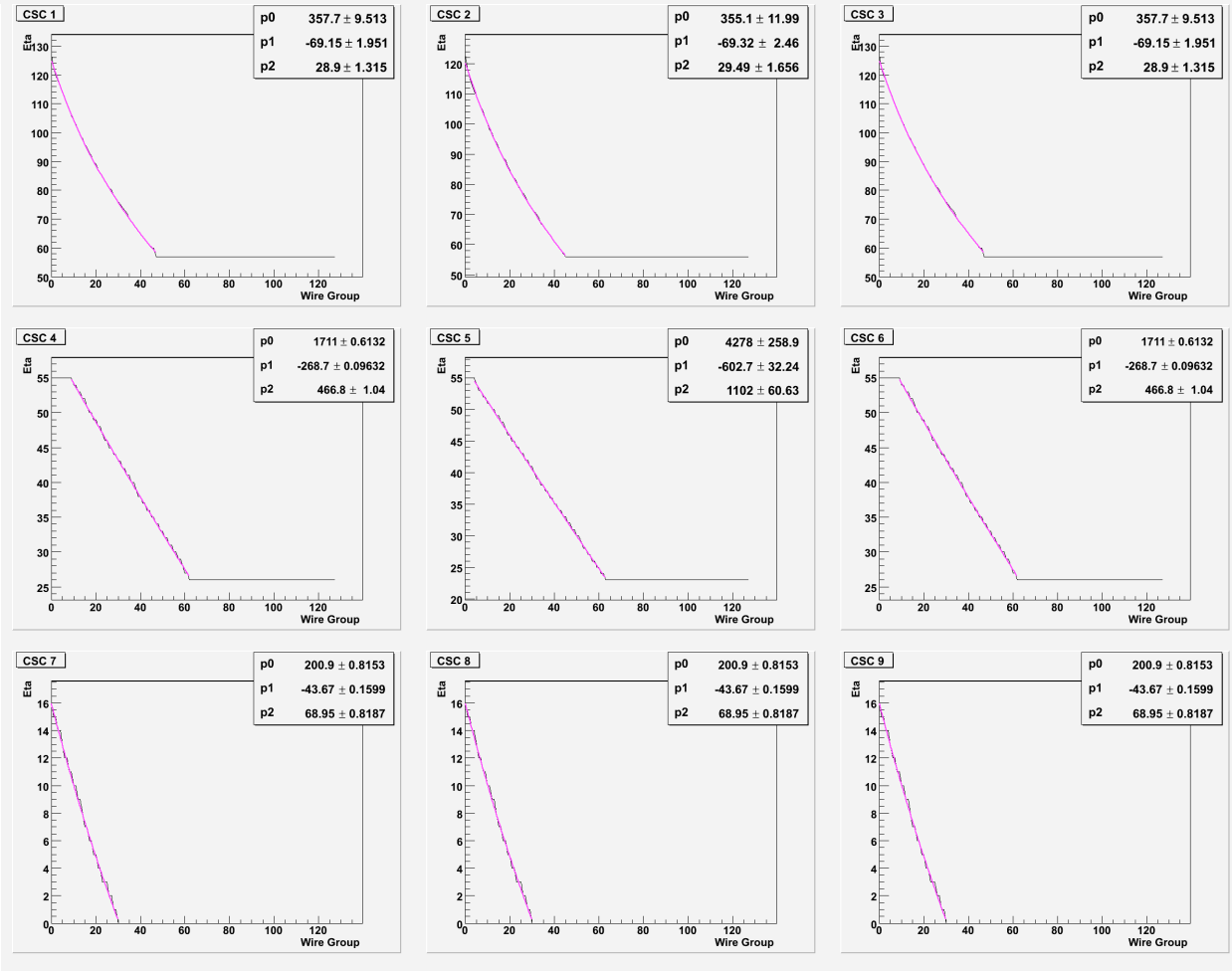
Figure 34: Global η ME for CSCs in endcap 1/sector 1/station 1a and a Local Phi of 0. The magenta line overlaying the data points is the parameterized curve fit obtained by fitting equation 4 to these data.